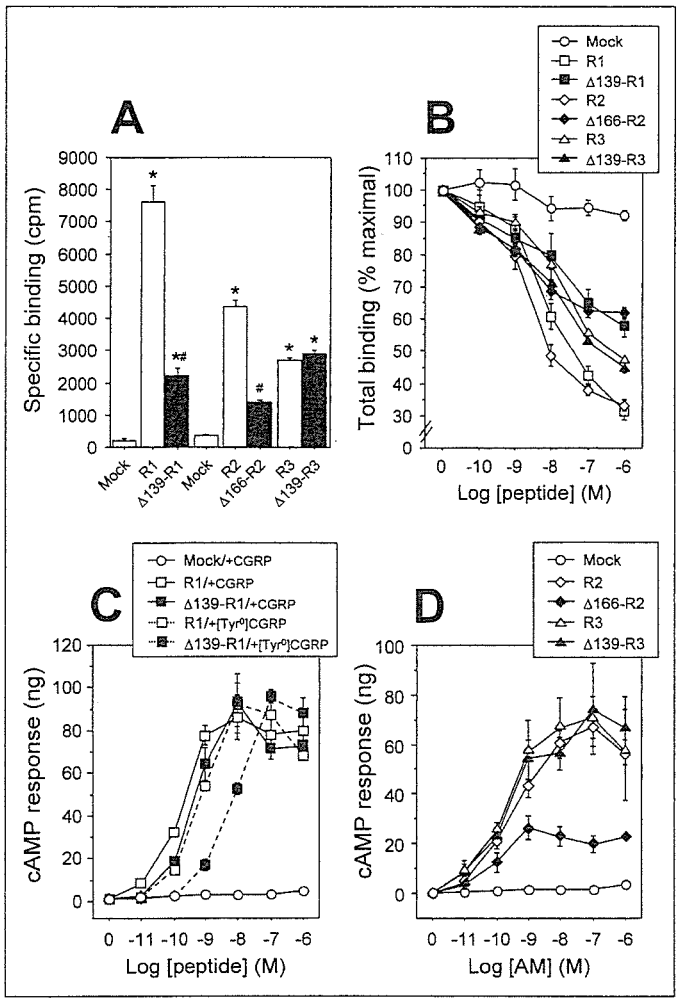


FIGURE 3. **Effects of hRAMP C-terminal deletion on agonist binding and evoked cAMP production in HEK-293 cells stably expressing hCRLR.** *A*, specific binding of $^{125}$I-h$\alpha$CGRP and $^{125}$I-hAM. HEK-293 cells expressing CRLR-GFP were transiently transfected with empty vector (*Mock*) or the indicated V5-RAMP or deletion mutant, after which the cells were incubated for 5 h at 4 °C with $^{125}$I-$\alpha$CGRP (100 pM) or $^{125}$I-AM (20 pM) in the presence or absence of 1 $\mu$M unlabeled $\alpha$CGRP or AM. *Bars* represent means ± S.E. of three experiments. *, $p < 0.002$ *versus* Mock; #, $p < 0.001$ *versus* corresponding wild-type V5-RAMP. *B*, displacement of radioligand. Cells were transfected and radiolabeled as in *A* either alone or with the indicated concentration of unlabeled ligand ($\alpha$CGRP or AM). *Bars* represent means ± S.E. of three experiments. *C* and *D*, evoked cAMP production. After transient transfection of V5-RAMPs and the corresponding deletion mutants, cells were exposed to the indicated concentrations of $\alpha$CGRP, [Tyr$^0$]$\alpha$CGRP, or AM for 15 min at 37 °C and then lysed. The resultant lysates were analyzed for cAMP content. *Bars* represent means ± S.E. of three experiments.

$^{125}$I-AM to CRLR-GFP-expressing cells, whereas cotransfection of Δ166-RAMP2 did not. In this case, the reduced binding could be due to reduced surface delivery of the mutant receptors (Fig. 2). Finally, deletion of the RAMP3 C-tail had no effect on specific $^{125}$I-AM binding.

Fig. 3*B* shows a set of $^{125}$I-[Tyr$^0$]$\alpha$CGRP and $^{125}$I-AM competition curves for the wild-type and mutant receptors. The $IC_{50}$ values derived from the curves obtained with cotransfection of Δ139-RAMP1 or Δ166-RAMP2 were both >1000 nM, which is much higher than those for RAMP1 and -2 (43.0 and 12.2 nM, respectively). By contrast, the $IC_{50}$ values obtained with expression of RAMP3 or Δ139-RAMP3 were within the same order of magnitude (560 and 257 nM, respectively).

We then further characterized the mutant receptors by measuring agonist-induced intracellular cAMP accumulation (Fig. 3, *C* and *D*). $\alpha$CGRP and AM elicited little or no cAMP production in HEK-293 cells expressing CRLR-GFP alone, indicating that the stable transfectants used in this study express no functional RAMP proteins. In cells coexpressing RAMP1 and CRLR-GFP, by contrast, $\alpha$CGRP ($EC_{50}$ = 0.18 nM) elicited marked increases in cAMP (Fig. 3*C*). In cells expressing Δ139-RAMP1 with CRLR-GFP, the $EC_{50}$ for $\alpha$CGRP was increased only a little, as compared with RAMP1 (to 0.49 nM), and the maximal responses were also similar to those seen with RAMP1 (Fig. 3*C*). Interestingly, the responses to [Tyr$^0$]$\alpha$CGRP by cells expressing CRLR-GFP/Δ139-RAMP1 ($EC_{50}$ = 8.5 nM) were significantly smaller than those seen in cells expressing CRLR-GFP/RAMP1 ($EC_{50}$ = 0.79 nM). In cells transfected with RAMP2, AM elicited significant increases in cAMP ($EC_{50}$ = 0.38 nM), but these responses were diminished by 62.1% in cells transfected with Δ166-RAMP2, although there was no significant change in $EC_{50}$ (0.16 nM) (Fig. 3*D*). AM-evoked cAMP production did not significantly differ in cells expressing RAMP3 or Δ139-RAMP3 ($EC_{50}$ = 0.41 and 0.20 nM, respectively) (Fig. 3*D*). That the cAMP production elicited via the respective receptors largely paralleled the profile of radioligand binding (Fig. 3, *A* and *B*) suggests that the C-tails of RAMP1 and -3 have little or no involvement with agonist binding and signaling.

We previously quantified the internalization and recycling of AM receptors (CRLR/RAMP heterodimers) using radioligand binding assays; however, interpretation of those experiments was complicated by the high degree of nonspecific AM binding, which reflected the highly hydrophobic and basic nature of the native peptide (1, 10, 11). In the present study, therefore, we used FACS to evaluate agonist-mediated internalization and recycling of wild-type and mutant CRLR-GFP/RAMP heterodimers. Fig. 4*A* shows the receptor internalization induced by 1 $\mu$M $\alpha$CGRP- or AM. Exposure to the appropriate agonist elicited rapid declines in cell surface expression of wild-type CRLR-GFP/RAMP1 and -3 that led to 40–60% reductions in signal strength within 2 h and to 90% reduction in cell surface CRLR-GFP/RAMP2 within 30 min. Heterodimers composed of CRLR-GFP plus Δ139-RAMP1 or Δ166-RAMP2 tended to be internalized somewhat less efficiently, whereas internalization of the CRLR-GFP/Δ139-RAMP3 heterodimer was markedly enhanced. Notably, these phenomena occurred with no changes in cell surface CRLR-GFP expression or AM binding and signaling (Figs. 2 and 3).

The dose dependence of the agonist-evoked receptor internalization is illustrated in Fig. 4*B*. $\alpha$CGRP elicited equivalent dose-dependent internalization of CRLR-GFP/RAMP1 and CRLR-GFP/Δ139-RAMP1. AM dose-dependently induced RAMP2-mediated internalization of CRLR-GFP, which was more efficient than RAMP1-mediated internalization. And Δ166-RAMP2 mediated internalization of CRLR-GFP even more efficiently than did wild-type RAMP2, although the basal surface expression of CRLR-GFP/Δ166-RAMP2 was much lower (Fig. 2*A*). Δ139-RAMP3-mediated internalization of CRLR-GFP only differed from that mediated by wild-type RAMP3 at high AM concentrations (100 nM and 1 $\mu$M), at which time internalization of the mutant was more efficient.

*Progressive Truncation of the C-Tails of hRAMP2 and -3*—The results presented so far show that for hRAMP1, the C-tail is not necessary for cell surface delivery and internalization of CRLR (Figs. 2 and 4). For hRAMP2 and -3, by contrast, the respective C-tails do appear to be involved in determining the surface expression and internalization kinetics of CRLR.

To determine more precisely which sites on the C-tails of hRAMP2 and -3 regulate the cellular trafficking of CRLR/RAMP heterodimers, we constructed a group of progressive C-tail truncation mutants (Fig. 1) and then transfected each RAMP construct into HEK-293 cells stably expressing CRLR-GFP. When Δ166- or Δ167-RAMP2 was individually transfected into HEK-293 cells, its transfection efficiency (~15%) was

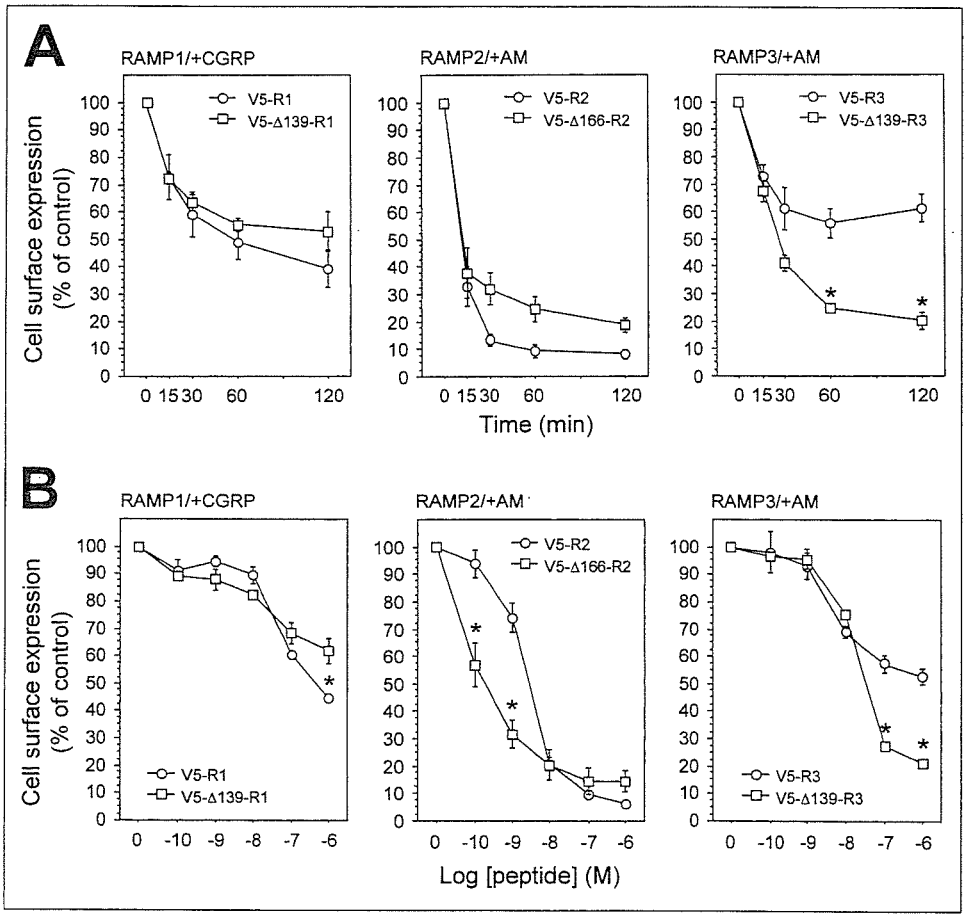


FIGURE 4. **FACS analysis of the time course of agonist-induced internalization of hCRLR with hRAMPs or their C-terminal deletion mutants.** *A*, time-dependent loss of surface CRLR/RAMP heterodimers. HEK-293 cells stably expressing CRLR-GFP were transiently transfected with V5-RAMPs or their C-terminal deletion mutants and then treated with 1 $\mu$M $\alpha$CGRP or AM for the indicated times. Cell surface expression of each construct was estimated by flow cytometry. The *symbols* represent means ± S.E. of three independent experiments; *, $p < 0.006$ *versus* control. *B*, agonist-evoked internalization of hCRLR with hRAMPs or their deletion mutants. Each transfectant was incubated for 60 min with the indicated concentrations of $\alpha$CGRP or AM. Cell surface expression of each construct was estimated by flow cytometry. *Symbols* represent means ± S.E. of three independent experiments; *, $p < 0.03$ *versus* control.

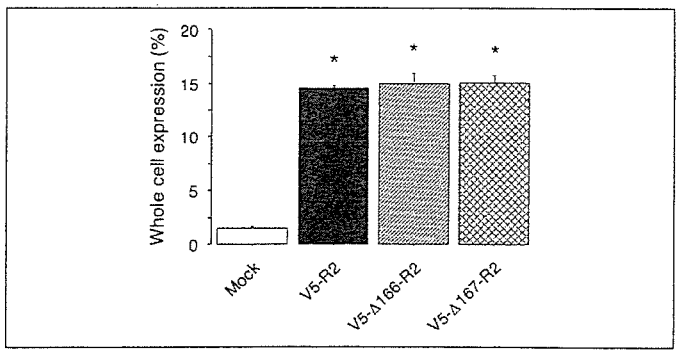


FIGURE 5. **FACS analysis of whole cell expression of hRAMP2 and its truncation mutants.** The indicated RAMP constructs were transiently transfected into HEK-293 cells. Forty-eight hours after transfection, cells were permeabilized with IntraPrep™ reagent and then incubated for 15 min at room temperature with anti-V5-FITC antibody; mock incubation with the antibody served as the control. Whole cell expression of each construct was estimated by flow cytometry. The *symbols* represent means ± S.E. of three independent experiments; *, $p < 0.001$ *versus* control.

comparable with that for wild-type RAMP2 (Fig. 5). Moreover, immunocytochemical analysis showed that almost all of both mutants remained in the ER, representing a pool of newly synthesized molecules not yet transported to the cell surface (Fig. 6). Although they were transfected into CRLR-GFP-expressing cells, however, Δ166- and Δ167-RAMP2 largely failed to transport CRLR-GFP to the cell surface, resulting in significant reductions in specific $^{125}$I-AM binding and AM-evoked cAMP production (Table 1). This suggests that the 168th and 169th amino acids (SK sequence) of RAMP2 are important for cell surface delivery of CRLR. The reason for the discrepancy between the $IC_{50}$ and $EC_{50}$ remains unclear, however. By contrast, Δ168- and Δ169-RAMP mediated substantially greater levels of cell surface CRLR-GFP expression, so that AM binding and signaling were equivalent to that seen with wild-type RAMP2 (Table 1). All of the RAMP3 truncation mutants appeared together with CRLR-GFP at the cell surface (Fig. 6*A*), and the resultant receptors showed AM binding and signaling that was comparable with that seen with wild-type RAMP3 (Table 1).

Among the RAMP2 mutants, Δ166 significantly reduced internalization of CRLR-GFP (Fig. 7). Conversely, the Δ139- and Δ140-RAMP3 mutants mediated significantly greater CRLR-GFP internalization than wild-type RAMP3 (Fig. 7). Such increases were not seen with Δ141-RAMP3, and CRLR-GFP internalization mediated by Δ142, Δ143, and Δ144 was equal to that seen with wild-type RAMP3. Thus, the presence of amino acids 141 and 142 (SK sequence) of RAMP3 leads to significant decreases in CRLR internalization.

*Characteristics of hRAMP C-tail Chimeras*—The SK sequence is highly conserved in the C-tails of all three hRAMPs (Fig. 1) as well as in RAMP isoforms from other species (17). We therefore tested whether exchanging C-tails would affect the cellular trafficking of CRLR-GFP. Given that hRAMP2 promoted CRLR internalization more effectively than other hRAMP isoforms did and that there were no differences in CRLR surface delivery and internalization by hRAMP1 and -3, we constructed four RAMP chimeras (RAMP1/2, -2/1, -2/3, and -3/2) by taking advantage of unique restriction sites that enabled us to generate four hybrid genes. These RAMP chimeras were then transiently transfected into HEK293 cells stably expressing CRLR-GFP and characterized by FACS analysis. As shown in Table 2, cell surface expression and evoked CRLR-GFP internalization of all four chimeras was comparable with

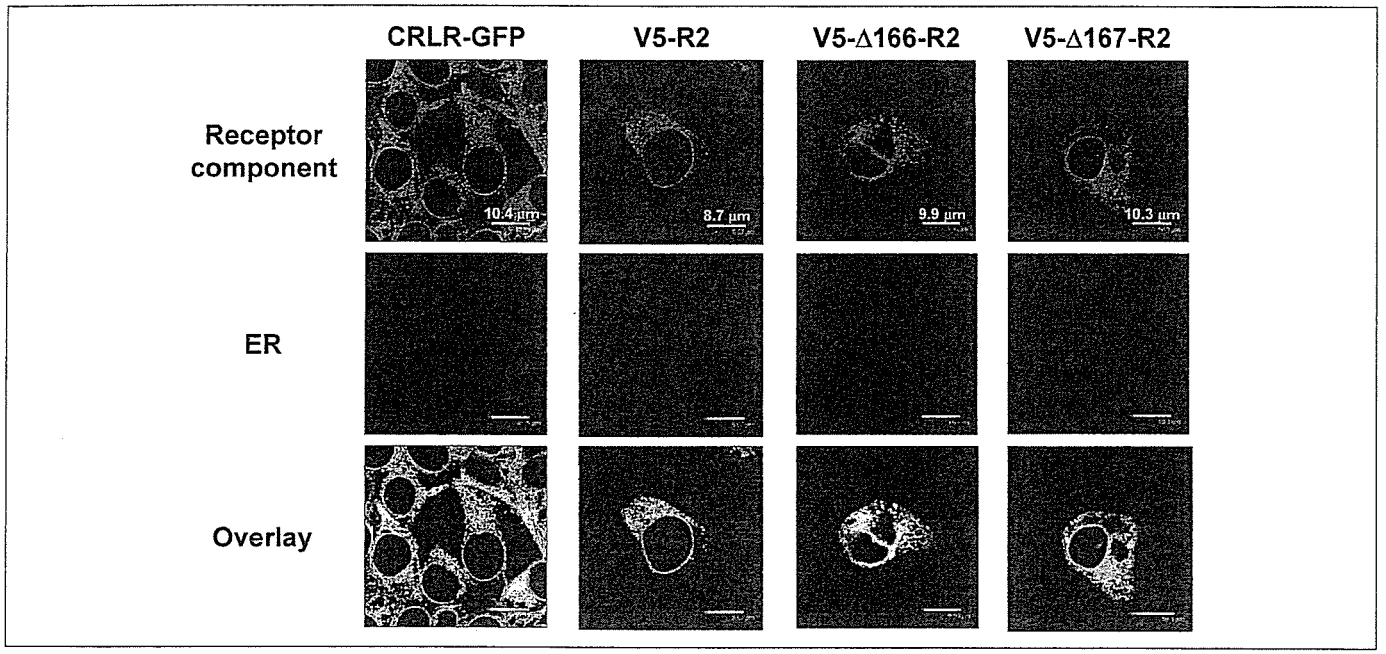


FIGURE 6. **Intracellular localization of V5-hRAMP2 and its truncation mutants.** The indicated RAMP2 constructs were transiently transfected into HEK-293 cells, after which their subcellular distribution was assessed by confocal microscopy in permeabilized cells using anti-V5-FITC antibody. Calnexin (for the ER) was visualized using the appropriate secondary antibody (Alexa Fluor® 594). Co-localization with the ER marker was determined by overlay of the images (*lower panels*). HEK-293 cells stably expressing CRLR-GFP served as the control for co-localization of CRLR-GFP and the ER (*left panels*). *Bar*, ~10 μm.

**TABLE 1**

**Characterization of HEK-293 cells expressing CRLR-GFP and progressive V5-RAMP2 and -3 truncation mutants**

The indicated RAMP constructs were transiently transfected into CRLR-GFP-expressing HEK-293 cells. Surface expression of each construct was estimated by flow cytometry. The results represent the means ± S.E. of three independent experiments.

| | Cell surface expression (% V5-RAMP2 or -3) | $^{125}$I-AM binding | | AM-evoked cAMP production | |
|---|---|---|---|---|---|
| | | $IC_{50}$ | Specific binding (% V5-RAMP2 or -3) | $EC_{50}$ | Maximal responses (% V5-RAMP2 or -3) |
| | % | nM | % | nM | % |
| V5-RAMP2 (R2) | 100 | 12.2 ± 5.0 | 100 | 0.38 ± 0.14 | 100 |
| V5-Δ166-R2 | 14.6 ± 1.5[a] | >1000 | 31.8 ± 1.4[a] | 0.16 ± 0.07 | 37.9 ± 4.7[a] |
| V5-Δ167-R2 | 29.0 ± 2.3[a] | >1000 | 48.0 ± 2.9[a] | 0.21 ± 0.09 | 52.3 ± 1.8[a] |
| V5-Δ168-R2 | 61.7 ± 5.5 | 13.7 ± 5.3 | 98.4 ± 7.2 | 0.26 ± 0.22 | 73.8 ± 20.5 |
| V5-Δ169-R2 | 83.6 ± 7.8 | 12.9 ± 3.5 | 95.8 ± 3.9 | 0.10 ± 0.06 | 87.8 ± 19.3 |
| V5-Δ172-R2 | 55.9 ± 8.1 | 18.0 ± 6.0 | 83.1 ± 2.4[a] | 0.24 ± 0.04 | 61.5 ± 4.9 |
| V5-RAMP3 (R3) | 100 | 560 ± 100 | 100 | 0.41 ± 0.25 | 100 |
| V5-Δ139-R3 | 89.3 ± 6.0 | 257 ± 49 | 107 ± 4.3 | 0.20 ± 0.08 | 93.8 ± 12.1 |
| V5-Δ140-R3 | 79.7 ± 5.3 | 687 ± 70 | 93.9 ± 1.7 | 2.50 ± 1.49 | 91.0 ± 5.7 |
| V5-Δ141-R3 | 89.1 ± 11.6 | 317 ± 73 | 114 ± 1.3[a] | 0.30 ± 0.14 | 116 ± 7.5 |
| V5-Δ142-R3 | 79.4 ± 9.7 | 483 ± 193 | 114 ± 4.5 | 0.98 ± 0.31 | 101 ± 8.6 |
| V5-Δ143-R3 | 84.0 ± 12.8 | 386 ± 307 | 111 ± 11.4 | 0.38 ± 0.21 | 113 ± 21.6 |
| V5-Δ144-R3 | 78.2 ± 10.3 | 383 ± 105 | 114 ± 6.1 | 0.13 ± 0.09 | 102 ± 12.1 |

[a] $p < 0.03$ *versus* corresponding control (V5-RAMP2 or -3).

that seen with the respective wild-type RAMPs. Thus, exchanging C-tails did not affect RAMP-mediated surface delivery or internalization of CRLR.

*Effect of hRAMP C-tail Deletion on Receptor Recycling*—For recycling studies, cells were pretreated with 10 μg/ml cycloheximide and 10 μg/ml brefeldin A to respectively inhibit *de novo* protein synthesis and cause disassembly of the Golgi apparatus (29); neither of these reagents had any effect of their own on CGRP- or AM-induced internalization of CRLR-GFP/RAMPs (data not shown). Subsequent treatment of cells with 1 μM αCGRP or AM for 60 min elicited a loss of cell surface receptors that persisted for at least 2 h after washing out the ligands (Fig. 8*A*). Very similar results were seen with Δ139-RAMP1, Δ166-RAMP2, and Δ139-RAMP3, suggesting the RAMP C-tails are not involved in lysosomal sorting of CRLR or the binding of protein(s) that determine the fate of internalized receptors.

*Internalization and Recycling of $AM_2$ Receptors in Cells Cotransfected with hNSF*—It was recently shown that, unlike NHERF, NSF contains no recognizable PDZ domains (30) but nonetheless interacts with the PDZ motif of hRAMP3, enabling internalized $AM_2$ receptors to undergo slow recycling (18). Conversely, NSF enhances β-arrestin 1-mediated $\beta_2$-AR internalization (31). Notably, although rat and mouse RAMP3 C-tails contain a RLL sequence instead of a PDZ motif, NSF also promotes recycling of these CRLR/RAMP3 heterodimers (18). With the aim of better understanding the role of NSF in $AM_2$ receptor trafficking, in the present study, we tested whether the reported effects of hNSF on CRLR/RAMP3 trafficking are reproduced in HEK-293 cells endogenously expressing hNSF and in hNSF transfectants.

We first confirmed that NSF was indeed endogenously expressed in HEK-293 cells by identifying both NSF mRNA and protein in the

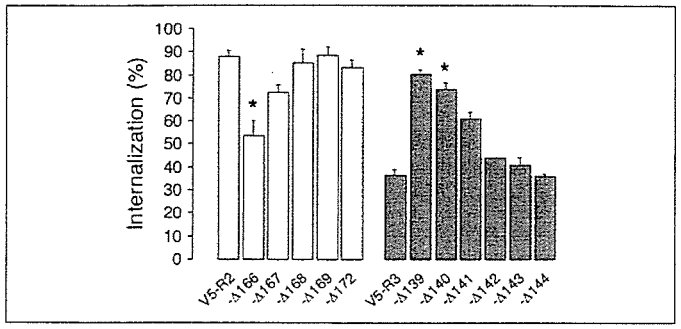


FIGURE 7. **FACS analysis of internalization of hCRLR with progressive hRAMP2 and -3 truncation mutants.** The indicated RAMP constructs were transiently transfected into CRLR-GFP-expressing HEK-293 cells. Surface expression of each construct was estimated by flow cytometry before and after exposing cells to 1 $\mu$M AM for 60 min. The results represent the means ± S.E. of three independent experiments; *, $p < 0.003$ *versus* corresponding control (V5-RAMP2 or -3).

**TABLE 2**

**FACS analysis of cell surface delivery and internalization of CRLR-GFP and V5-RAMP chimeras in which the C-tails were exchanged among the three RAMPs**

The indicated V5-RAMPs or their chimeras were transiently transfected into CRLR-GFP-expressing HEK-293 cells. Surface expression of each construct was estimated by flow cytometry before and after exposing cells to 1 $\mu$M $\alpha$CGRP or AM for 60 min. The results represent the means ± S.E. of three independent experiments.

| | Cell surface expression | Internalization |
|---|---|---|
| | % | % |
| V5-RAMP1 | 51.8 ± 3.7 | 50.0 ± 4.3 |
| V5-RAMP2 | 23.2 ± 2.7 | 94.5 ± 1.6 |
| V5-RAMP3 | 46.3 ± 4.8 | 35.5 ± 1.8 |
| V5-RAMP1/2 | 49.7 ± 5.6 | 53.7 ± 7.2 |
| V5-RAMP2/1 | 25.8 ± 2.3 | 91.8 ± 0.4 |
| V5-RAMP2/3 | 19.5 ± 1.4 | 88.2 ± 1.2 |
| V5-RAMP3/2 | 44.9 ± 6.1 | 36.7 ± 3.8 |

cells (Fig. 8, *B* and *C*). Thereafter, we determined that the levels of the transcript were unaffected by transfection of CRLR-GFP alone or together with V5-RAMP3 (Fig. 8*D*). When NSF was transfected into otherwise untransfected HEK-293 cells and into CRLR-GFP transfectants, levels of its transcript were markedly higher than their endogenous levels in both (Fig. 8*B*). In those cases, Western analysis of NSF protein yielded a single, strong 76-kDa band that was identical to the band obtained when endogenous NSF was probed (Fig. 8*C*), which confirmed that our NSF transfection system worked appropriately. Exposure to 10 nM or 1 $\mu$M AM for 60 min induced a rapid decline in cell surface CRLR-GFP/V5-RAMP3 that persisted for at least 4 h after washing out the AM (Fig. 8*D*). Cotransfection of NSF had no effect on these internalization kinetics, and recycling of CRLR/RAMP3 heterodimers, if it occurred, was highly inefficient, even in the presence of abundant NSF (Fig. 8*D*).

## DISCUSSION

Since their discovery, there have been only a few reports addressing the functions of the respective C-tails of the three RAMP isoforms (17–19, 32, 33); more extensively studied have been their extracellular domains (11–13, 17, 32, 34, 35). Consequently, whereas nearly all highly conserved residues are known to play key roles in the function and trafficking of cell surface receptors, nothing is known about the functions of the highly conserved Ser and Lys resides within RAMP C-tails. In the present study, we showed that deleting the C-tail from RAMP3 (Δ139-RAMP3) significantly enhanced AM-induced CRLR-GFP internalization but did not affect the targeting of CRLR-GFP to the cell surface or AM binding and signaling. It is therefore unlikely that the truncation of RAMP3 promoted AM-induced conformational changes in the heterodimeric receptors that would alter the binding of AM and/or the interaction of the receptor with G proteins. On the other hand, like wild-type RAMP3, all of the tested RAMP3 truncation mutants that contained the SK sequence (Δ142-, Δ143-, and Δ144-RAMP3) mediated CRLR-GFP internalization less efficiently than those that did not (Δ139-, Δ140-, or Δ141-RAMP3). We also found that substituting the RAMP3 C-tail with the RAMP2 C-tail, which also contains a SK sequence, had no effect on the AM-induced CRLR-GFP internalization. Taken together, these results suggest that the SK sequence participates in the negative regulation of CRLR/RAMP3 internalization.

The Ser/Thr residues present in the C-tails of the three RAMP have been thought to be potential phosphorylation sites, but Hilairet *et al.* (6) showed that in HEK-293 cells overexpressing CRLR/RAMP heterodimers, agonists rapidly promote phosphorylation of CRLR but not RAMP. They also demonstrated that internalization of the heterodimeric receptors was dependent on $\beta$-arrestins (6). In the present study, complete removal of the respective RAMP C-tails did not diminish the maximal extent of internalization. It therefore seems unlikely that $\beta$-arrestins interact with the RAMP C-tails.

Similar in function to the SK sequence, a dileucine (LL) motif, which is conserved among GPCRs (36), is also present in the C-tail of RAMP3. This motif negatively regulates lutropin/choriogonadotropin receptor (LHR) internalization, since leucine-to-alanine mutations increased the agonist-stimulated internalization of the receptor (37). It is thought that the LL motif participates in protein sorting through direct interaction with two clathrin adaptor protein (AP) complexes, AP-1 and AP-2 (38–40), and the point mutations disrupted the interaction of the LHR with AP-2 at the plasma membrane (39). On the other hand, these mutations are believed to enhance the binding of $\beta$-arrestins to the LHR, thereby promoting bridge formation between $\beta$-arrestins and clathrin (37). We suggest that, instead of $\beta$-arrestins, the RAMP3 C-tail may interact with other intracellular proteins similar to LRP6, another GPCR accessory protein that interacts with axin and catinin (41).

We believe it is noteworthy that the hRAMP3 C-tail contains not only a LL sequence but also a type I PDZ binding sequence (see Fig. 1). Recently, NHERF-1 was found to interact with the PDZ motif of hRAMP3, resulting in complete inhibition of CRLR/RAMP3 internalization (33). In that case, NHERF-1 is thought to act by tethering surface $AM_2$ receptors to the actin cytoskeleton in a manner also seen with epidermal growth factor receptors (42). By contrast, NHERF-1 promotes the agonist-mediated recycling of $\beta_2$-ARs, which also have a PDZ motif (SLL) (30). The mechanism by which NHERF-1 exerts these differing effects on different GPCRs remains unknown. In the present study, three RAMP3 truncation mutants (Δ142-, Δ143-, and Δ144-RAMP3) and the RAMP3/2 chimera, all of which lack both the LL and PDZ sequences, failed to enhance the AM-induced CRLR-GFP internalization. However, this does not preclude the possibility that the level of endogenous NHERF-1 expression in HEK-293 cells used was insufficient to modulate the behavior of the overexpressed RAMP3.

We also showed that deleting the C-tail of RAMP2 impaired the targeting of the CRLR-GFP to the cell surface, thereby markedly reducing AM binding and signaling. Most of the newly synthesized Δ166-RAMP2 remained in the ER along with CRLR-GFP. By contrast, removing the C-tail from RAMP1 or -3 did not diminish surface delivery of the respective receptors. All of the RAMP2 mutants containing an SK sequence (Δ168-, Δ169-, and Δ172-RAMP2) showed better surface CRLR-GFP expression than was seen with Δ166-RAMP2, which lacked the SK sequence. Apparently, the SK sequence in the RAMP2 C-tail is involved in the proper membrane localization of the CRLR/RAMP2. To our knowledge, there have

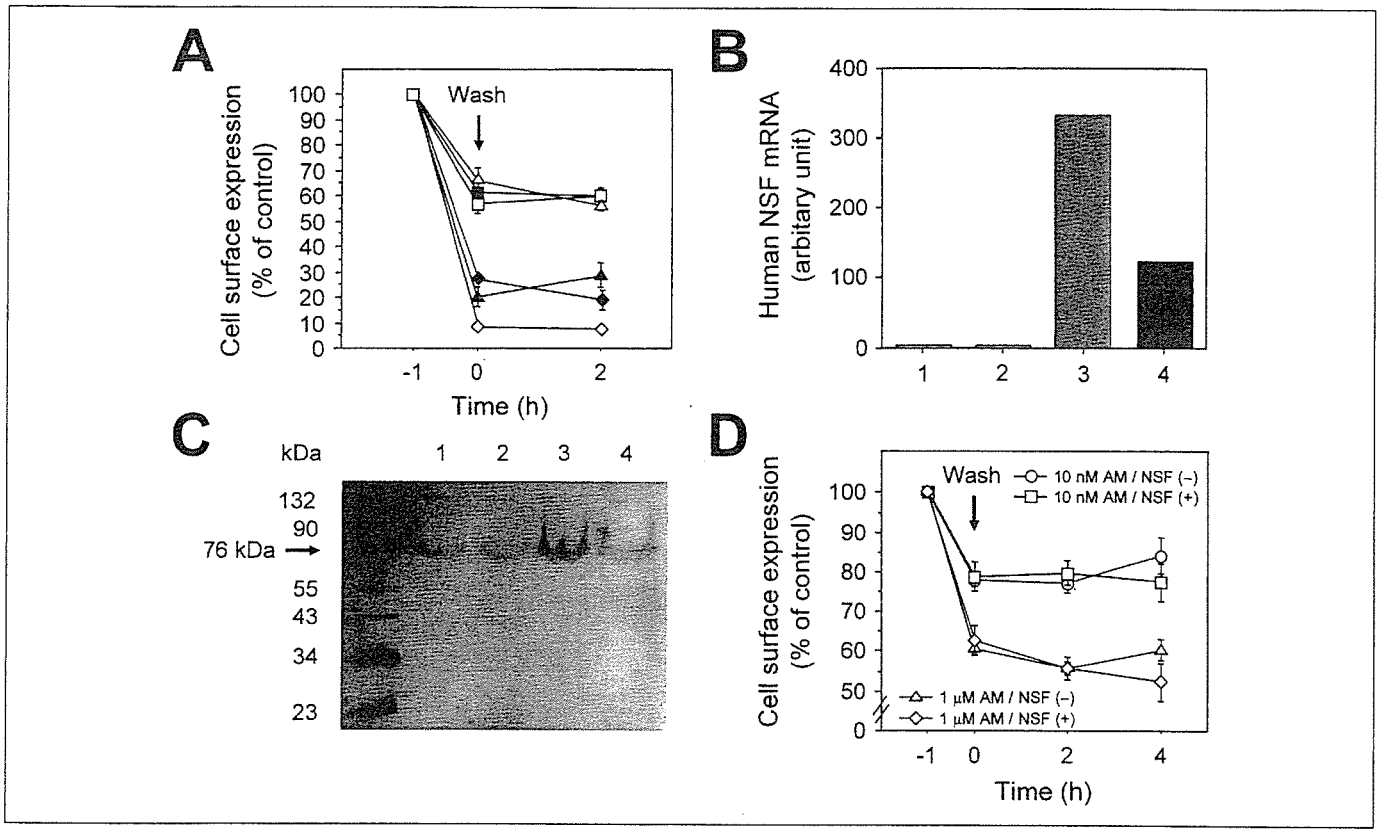


FIGURE 8. **The fates of internalized hCRLR and hRAMPs and their C-terminal deletion mutants.** *A*, FACS analysis of recycling of the internalized heterodimeric receptors. HEK-293 cells stably expressing CRLR-GFP were transiently transfected with each RAMP construct (*symbols* are the same as in Fig. *3B*), after which they were incubated for 60 min with 1 μM αCGRP or AM plus 10 μg/ml cycloheximide and 10 μg/ml brefeldin A. The cells were then washed with prewarmed PBS and labeled with the indicated antibodies. Cell surface expression of each construct was estimated by flow cytometry. *Bars* represent means ± S.E. of three independent experiments. *B*, endogenous and transiently transfected hNSF mRNA levels. *1*, intact HEK-293 cells; *2*, HEK-293 cells stably expressing CRLR-GFP; *3*, NSF-transfected HEK-293 cells; *4*, NSF-transfected HEK-293 cells stably expressing CRLR-GFP. Expression of NSF mRNA was assessed using real time quantitative PCR with the appropriate primers and probes. Levels of NSF mRNA were normalized to that of GAPDH mRNA, which served as an internal control. *Bars* represent the average of two experiments. *C*, Western analysis of endogenous NSF and overexpressed NSF in HEK-293 cells. Equal aliquots of protein (20 μg) were subjected to 10% SDS gel electrophoresis. *Lane 1*, cells expressing empty vector (*Mock*); *lane 2*, cells stably expressing CRLR-GFP; *lane 3*, cells transiently expressing NSF; *lane 4*, cells expressing both CRLR-GFP and NSF. The blots shown are representative of three independent experiments. *D*, FACS analysis of the recycling of CRLR and RAMP3 in the presence and absence of NSF. CRLR-GFP-expressing cells were transiently transfected with V5-RAMP3 plus empty vector or NSF, after which they were incubated for 60 min with 10 nM or 1 μM AM plus 10 μg/ml cycloheximide and 10 μg/ml brefeldin A. The cells were then treated as described in *A*. Cell surface expression of each construct was estimated by flow cytometry. The *symbols* represent means ± S.E. of three independent experiments.

been no studies on the relation between the SK sequence and surface delivery of other GPCRs, but the LL sequence in the C-tail of the $V_2$ vasopressin receptor was found to be crucial for ER-to-Golgi transfer of that receptor, presumably by helping establish a correct and transport-competent folding state (36). Similarly, RAMPs appear to mediate transport of the CRLR from the ER to the Golgi, since CRLR was restricted to the ER in the absence of RAMPs (6). It therefore seems likely that the SK sequence in the RAMP2 C-tail, but not that in the RAMP3 C-tail, is essential for the escape of CRLR from the ER. The mechanism underlying the differential effect of the SK sequence on the cellular trafficking of these two AM receptors remains to be determined.

There have been two studies on the effects of CGRP in HEK-293 cells coexpressing hCRLR with a hRAMP1 C-tail deletion mutant (19, 32). One found that the C-tail deletion resulted in a 1-order of magnitude reduction in CGRP-stimulated cAMP formation, but no data on CGRP binding were shown (19). In that case, the 140th residue Gln, but not the SK sequence, most likely determined the affinity of CGRP for the receptor. The other study found no significant changes in CGRP binding or signaling (32). Similarly, we found that deleting the C-tail of RAMP1 had little effect on receptor signaling, as reflected by CGRP-evoked cAMP production, although the binding profile we obtained differed from that obtained in the earlier study (32). This absence of a significant change in the potency of CGRP may indicate that there was little change in the internalization of CRLR-GFP. In contrast to the αCGRP responses, $^{125}$I-[Tyr$^0$]αCGRP binding to CRLR-GFP/Δ139-RAMP1 was much diminished. This discrepancy could be due in part to interference by the extra N-terminal tyrosine residue (Tyr$^0$). In any event, the contribution of the RAMP1 C-tail to CGRP potency is much smaller than that made by its extracellular domain (13, 17, 32, 34, 35).

Several earlier studies showed that internalized CRLR/RAMP heterodimers are trafficked to lysosomes for degradation (6, 10). It is now recognized that receptor ubiquitination is essential for proper trafficking to lysosomes (43). Indeed, our CRLR-GFP-transfected HEK-293 cells abundantly expressed endogenous ubiquitin, which attaches to lysine residues within the substrate proteins (data not shown). Nevertheless, truncation of RAMP C-tails that removed the Lys residues failed to promote recycling of CRLR-GFP. This raises the possibility that expression of intracellular proteins involved in mediating appropriate receptor recycling was inadequate in the HEK-293 cells used. NSF, like NHERF, is believed to enhance recycling of internalized receptors (44), and it was recently shown that NSF interacts with the PDZ motif of hRAMP3, enabling internalized $AM_2$ receptors to undergo slow recycling (18). Notably, although rat and mouse RAMP3 tails contain an RLL sequence instead of a PDZ motif, NSF also promoted recycling of CRLR/RAMP3 heterodimers

(18). In the present study, however, the cells abundantly expressed endogenous NSF, making it unlikely that poor expression of NSF underlies the trafficking of CRLR-GFP/RAMP3 to lysosomes without recycling. Even overexpression of NSF in these cells did not alter the AM-mediated trafficking of $AM_2$ receptors.

The rapid recycling pathway has been best studied and characterized for the $\beta_2$-AR, which has a PDZ motif in its C-tail (14, 15, 30) and which requires both NHERF and NSF for its recycling (30, 44). Indeed, among 59 representative seven-transmembrane segment GPCRs tested, NSF bound most strongly to the $\beta_2$-AR tail (44). However, a point mutation within the PDZ motif that disrupted the binding of NSF, but not that of NHERF, had no effect on $\beta_2$-AR recycling (30). In addition, the $\beta_1$-AR and cystic fibrosis transmembrane regulator each contain a C-terminal PDZ binding sequence (SKV and TRL, respectively) and undergo rapid recycling, despite their failure to bind NSF (30). Thus, NSF binding to GPCRs and RAMP3 is not required for recycling of proteins containing PDZ binding sequences.

In summary, our results indicate that the C-tails of hRAMP2 and -3 are involved in hCRLR surface delivery and internalization, respectively, and that the highly conserved SK sequence within their C-tails is a key determinant of the cellular behavior of the $AM_1$ and $AM_2$ receptors.

## REFERENCES


1. Kitamura, K., Kangawa, K., Kawamoto, M., Ichiki, Y., Nakamura, S., Matsuo, H., and Eto, T. (1993) *Biochem. Biophys. Res. Commun.* **192,** 553–560
2. Eto, T. (2001) *Peptides* **22,** 1693–1711
3. Poyner, D. R., Sexton, P. M., Marshall, I., Smith, D. M., Quirion, R., Born. W., Muff, R., Fischer, J. A., and Foord, S. M. (2002) *Pharmacol. Rev.* **54,** 233–246
4. McLatchie, L. M., Fraser, N. J., Main, M. J., Wise, A., Brown, J., Thompson, N., Solari, R., Lee, M. G., and Foord, S. M. (1998) *Nature* **393,** 333–339
5. Sexton, P. M., Albiston, A., Morfis, M., and Tilakaratne, N. (2001) *Cell Signal.* **13,** 73–83
6. Hilairet, S., Belanger, C., Bertrand, J., Laperriere, A., Foord, S. M., and Bouvier, M. (2001) *J. Biol. Chem.* **276,** 42182–42190
7. Kuwasako, K., Cao, Y-N., Nagoshi, Y., Kitamura, K., and Eto, T. (2004) *Peptides* **25,** 2003–2012
8. Nagoshi, Y., Kuwasako, K., Ito, K., Uemura, T., Kato, J., Kitamura, K., and Eto, T. (2002) *Eur. J. Pharmacol.* **450,** 237–243
9. Muff, R., Born, W., and Fischer, J. A. (2003) *Hypertens. Res.* **26,** 3–8
10. Kuwasako, K., Shimekake, Y., Masuda, M., Nakahara, K., Yoshida, T., Kitaura, M., Kitamura, K., Eto, T., and Sakata, T. (2000) *J. Biol. Chem.* **275,** 29602–29609
11. Kuwasako, K., Kitamura, K., Ito, K., Uemura, T., Yanagita, Y., Kato, J., Sakata, T., and Eto, T. (2001) *J. Biol. Chem.* **276,** 49459–49465
12. Kuwasako, K., Kitamura, K., Onitsuka, H., Uemura, T., Nagoshi, Y., Kato, J., and Eto, T. (2002) *FEBS Lett.* **519,** 113–116
13. Kuwasako, K., Kitamura, K., Nagoshi, Y., Cao Y-N., and Eto, T. (2003) *J. Biol. Chem.* **278,** 22623–22630
14. Koenig, J. A., and Edwardson, J. M. (1997) *Trends. Pharmacol. Sci.* **18,** 276–287
15. Krupnick, J. G., and Benovic, J. L. (1998) *Annu. Rev. Pharmacol. Toxicol.* **38,** 289–319
16. Ferguson, S. S. G. (2001) *Pharmacol. Rev.* **53,** 1–24
17. Hay, D. L., Poyner, D. R., and Sexton, P. M. (2006) *Pharmacol. Ther.* **109,** 173–197
18. Bomberger, J. M., Parameswaran, N., Hall, C. S., Aiyar, N., and Spielman, W. S. (2005) *J. Biol. Chem.* **280,** 9297–9307
19. Steiner, S., Muff, R., Gujer, R., Fischer, J. A., and Born, W. (2002) *Biochemistry* **41,** 11398–11404
20. Hicke, L., and Riezman, H. (1996) *Cell* **84,** 277–287
21. Roth, A. F., and Davis, N. G. (1996) *J. Cell Biol.* **134,** 661–674
22. Martin, N. P., Lefkowitz, R. J., and Shenoy, S. K. (2003) *J. Biol. Chem.* **278,** 45954–45959
23. Shenoy, S. K., and Lefkowitz, R. J. (2003) *J. Biol. Chem.* **278,** 14498–14506
24. Kuwasako, K., Cao, Y-N., Nagoshi, Y., Tsuruda, T., Kitamura, K., and Eto, T. (2004) *Mol. Pharmacol.* **65,** 207–213
25. Aiyar, N., Rand, K., Elshourbagy, N. A., Zeng, Z., Adamou, J. E., Bergsma, D. J., and Li, Y. (1996) *J. Biol. Chem.* **271,** 11325–11329
26. Guon, X.-M., Kobilka, T. S., and Kobilka, B. K. (1992) *J. Biol. Chem.* **267,** 21995–21998
27. Nagoshi, Y., Kuwasako, K., Cao, Y-N., Kitamura, K., and Eto, T. (2004) *Biochem. Biophys. Res. Commun.* **314,** 1057–1063
28. Cao, Y-N., Kuwasako, K., Kato, J., Yanagita, T., Tsuruda, T., Kawano, J., Nagoshi, Y., Chen, A. F., Wada, A., Suganuma, T., Eto, T., and Kitamura, K. (2005) *Biochem. Biophys. Res. Commun.* **332,** 866–872
29. Xu, J., and Tse, F. W. (1999) *J. Biol. Chem.* **274,** 19095–19102
30. Gage, R. M., Matveeva, E. A., Whiteheart, S. W., von Zastrow, M. (2005) *J. Biol. Chem.* **280,** 3305–3313
31. McDonald, P. H., Cote, N. L., Lin, F-T., Premont, R. T., Pitcher, J. A., and Lefkowitz, R. J. (1999) *J. Biol. Chem.* **274,** 10677–10680
32. Fitzsimmons, T. J., Zhao, X., and Wank, S. A. (2003) *J. Biol. Chem.* **278,** 14313–14320
33. Bomberger, J. M., Spielman, W. S., Hall, C. S., Weinman, E. J., and Parameswaran, N. (2005) *J. Biol. Chem.* **280,** 23926–23935
34. Fraser, N. J., Wise, A., Brown, J., McLatchie, L. M., Main, M. J., and Foord, S. M. (1999) *Mol. Pharmacol.* **55,** 1054–1059
35. Hilairet, S., Foord, S. M., Marshall, F. H., and Bouvier, M. (2001) *J. Biol. Chem.* **276,** 29575–29581
36. Schulein, R., Hermosilla, R., Oksche, A., Dehe, M., Wiesner, B., Krause, G., and Rosenthal, W. (1998) *Mol. Pharmacol.* **54,** 525–535
37. Nakamura, K., and Ascoli, M. (1999) *Mol. Pharmacol.* **56,** 728–736
38. Dietrich, J., Kastrup, J., Nielsen, B. L., Odum, N., and Geisler, C. (1997) *J. Cell Biol.* **138,** 271–281
39. Kirchhausen, T., Bonifacino, J. S., and Riezman, H. (1997) *Curr. Opin. Cell Biol.* **9,** 488–495
40. Rapoport, I., Chen, Y-C., Cupers, P., Shoelson, S. E., and Kirchhausen, T. (1998) *EMBO J.* **17,** 2148–2155
41. Tamai, K., Semenov, M., Kato, Y., Spokony, R., Liu, C., Katsuyama, Y., Hess, F., Saint-Jeannet, J. P., and He, X. (2000) *Nature* **407,** 530–535
42. Lazar, C. S., Cresson, C. M., Lauffenburger, D. A., and Gill, G. N. (2004) *Mol. Biol. Cell* **15,** 5470–5480
43. Wojcikiewicz, R. J. H. (2004) *Trends Pharmacol. Sci.* **25,** 35–41
44. Heydorn, A., Sondergaard, B. P., Ersboll, B., Holst, B., Nielsen, F. C., Haft, C. R., Whistler, J., and Schwartz, T. W. (2004) *J. Biol. Chem.* **279,** 54291–54303

Available online at www.sciencedirect.com
ScienceDirect
Journal of Molecular and Cellular Cardiology 42 (2007) 88–97
Journal of Molecular and Cellular Cardiology
www.elsevier.com/locate/yjmcc

Original article

# Transplantation of mesenchymal stem cells attenuates myocardial injury and dysfunction in a rat model of acute myocarditis

Shunsuke Ohnishi [a,*,1], Bobby Yanagawa [a,1], Koichi Tanaka [a], Yoshinori Miyahara [a], Hiroaki Obata [a,b], Masaharu Kataoka [a], Makoto Kodama [b], Hatsue Ishibashi-Ueda [c], Kenji Kangawa [d], Soichiro Kitamura [e], Noritoshi Nagaya [a,*]

[a] *Department of Regenerative Medicine and Tissue Engineering, National Cardiovascular Center Research Institute, Fujishirodai 5-7-1, Osaka 565-8565, Japan*
[b] *Division of Cardiology, Niigata University Graduate School of Medical and Dental Sciences, Niigata, Japan*
[c] *Department of Pathology, National Cardiovascular Center, Osaka, Japan*
[d] *Department of Biochemistry, National Cardiovascular Center Research Institute, Osaka, Japan*
[e] *Department of Cardiovascular Surgery, National Cardiovascular Center, Osaka, Japan*

Received 11 May 2006; received in revised form 29 August 2006; accepted 2 October 2006
Available online 13 November 2006

**Abstract**

Acute myocarditis is a non-ischemic inflammatory disease of the myocardium for which there is currently no specific treatment. We have previously shown that mesenchymal stem cells (MSC) can ameliorate heart injury during acute ischemia and in dilated cardiomyopathy; however, the therapeutic potential in acute myocarditis is unclear. In this study, we investigated the ability of MSC to attenuate myocardial injury and dysfunction during the acute phase of experimental myocarditis. Ten-week-old male Lewis rats were injected with porcine myosin to induce myocarditis. Cultured MSC ($3 \times 10^6$ cells/rat) were injected intravenously 7 days after myosin injection. At 3 weeks, myosin injection resulted in severe inflammation and significant deterioration of cardiac function. MSC transplantation attenuated increases in CD68-positive inflammatory cells and monocyte chemoattractant protein-1 (MCP-1) expression in myocardium, and improved cardiac function in this model. Furthermore, myocardial capillary density was higher in myocarditis tissue, and was further increased by MSC transplantation. *In vitro*, cultured adult rat cardiomyocytes were injured in response to MCP-1, whereas this effect was attenuated by MSC-derived conditioned medium, suggesting cardioprotective effects of MSC acting in a paracrine manner. MSC transplantation attenuated myocardial injury and dysfunction in a rat model of acute myocarditis, at least in part through paracrine effects of MSC.


*Keywords:* Acute myocarditis; Mesenchymal stem cell; Paracrine effect; Cytokine; Cell death

## 1. Introduction

Acute myocarditis is a non-ischemic heart disease characterized by myocardial inflammation and edema. This disease is associated with rapidly progressive heart failure, arrhythmias and sudden death [1,2]. Although the early evidence for efficacy of immunoglobulin and interferon therapy appears promising, these results have yet to be demonstrated in randomized or controlled clinical trials. The current options are restricted to supportive care for heart failure or arrhythmias. The lack of specific treatment and the potential severity of the illness emphasize the importance of novel and effective therapeutic strategies for myocarditis.

Mesenchymal stem cells (MSC) are multipotent stem cells present in adult tissues, and have the ability to differentiate into a variety of lineages, including vascular smooth muscle cells, endothelial cells and cardiomyocytes [3,4]. We have previously reported that bone marrow-derived MSC engrafted in experimental myocardial infarction expressed both cardiac and endothelial phenotypes in the heart, and further increased capillary density and decreased the infarct size [5]. Moreover, we have recently demonstrated that monolayered MSC derived from adipose tissue reversed wall thinning in the scar area and improved cardiac function in rats with myocardial infarction [6]. The cardioprotective effects of MSC are known to be mediated

* Corresponding authors. Tel.: +81 6 6833 5012; fax: +81 6 6833 9865.
*E-mail addresses:* sonsihi@ri.ncvc.go.jp (S. Ohnishi), nnagaya@ri.ncvc.go.jp (N. Nagaya).
[1] Drs Ohnishi and Yanagawa contributed equally to this study.

0022-2828/$ - see front matter © 2006 Elsevier Inc. All rights reserved.
doi:10.1016/j.yjmcc.2006.10.003

not only by their differentiation into vascular cells and cardiomyocytes, but also by their ability to supply large amounts of angiogenic, anti-apoptotic and mitogenic factors [5–7]. These findings suggest the therapeutic potential of MSC for heart failure. However, whether intravenously transplanted MSC attenuate myocardial inflammation and cardiac dysfunction in acute myocarditis remains unknown.

In the present study, we used porcine myosin-induced acute myocarditis in Lewis rats. This model closely resembles human giant cell myocarditis, a frequently fatal disorder characterized by multinucleated giant cells in the myocardium [8]. To examine the therapeutic potential of MSC in the acute phase of myocarditis, MSC were intravenously injected into rats 7 days after myosin injection.

Thus, the purposes of this study were 1) to investigate whether intravenous transplantation of MSC improves cardiac function and pathological findings including myocardial inflammation in rats with myosin-induced myocarditis, and 2) to investigate the underlying mechanisms responsible for the effects of MSC.

## 2. Materials and methods

### 2.1. Animals

Ten-week-old male Lewis rats (Japan SLC, Hamamatsu, Japan) were used in all experiments, and were maintained in our animal facilities. The experimental protocols were approved by The Animal Care Committee of the National Cardiovascular Center.

### 2.2. Preparation of cardiac myosin

Purified cardiac myosin from the ventricular muscle of pig hearts was prepared according to a procedure described previously [8]. The antigen was dissolved at a concentration of 20 mg/ml in phosphate-buffered saline (PBS) containing 0.3 M KCl, mixed with an equal volume of complete Freund's adjuvant containing 11 mg/ml *Mycobacterium tuberculosis* (Difco Laboratories, Sparks, MD, USA). Rats were anesthetized with an intraperitoneal injection of 20 mg/kg sodium pentobarbital, and 0.1 ml of the antigen-adjuvant emulsion was injected into the each footpad.

### 2.3. Acute myocarditis model

Forty-five rats were randomly divided into three groups and received the following treatment: 1) 0.2 ml saline and sham surgery (Sham group, $n=15$), 2) 0.2 ml cardiac myosin antigen and sham surgery (MyoC group, $n=15$), and 3) 0.2 ml cardiac myosin followed by MSC transplantation 7 days post-myosin injection (MyoC+MSC group, $n=15$). Rats were weighed and observed daily for signs of morbidity and for death.

### 2.4. Preparation and transplantation of bone marrow-derived MSC

MSC were prepared as described previously [5]. Briefly, bone marrow cells were isolated by flushing out the femoral and tibial cavities with PBS, and plated onto 10-cm dishes in complete culture medium: Dulbecco's Modified Eagle's Medium (DMEM), 15% fetal bovine serum, 100 U/ml penicillin and 100 μg/ml streptomycin. Five days after plating, non-adherent cells were removed, and adherent cells were further propagated for 4 to 5 passages.

Seven days after myosin injection, MSC ($3\times10^6$ cells) or vehicle (0.9% saline) was intravenously administered via the jugular vein. Sham rats also received saline administration but without myosin injection.

### 2.5. Hemodynamic studies

Hemodynamic studies were performed on day 21 post-myosin injection. Anesthesia was maintained with an intraperitoneal injection of 20 mg/kg sodium pentobarbital, and a 1.5 Fr micromanometer-tipped catheter was placed in the left ventricle through the right carotid artery (Millar Instruments, Houston, TX, USA). Heart rate (HR) was also monitored by electrocardiography. HR, mean arterial pressure (MAP), left ventricular systolic pressure (LVSP), left ventricular end-diastolic pressure (LVEDP), maximum $dP/dt$ (Max $dP/dt$) and minimum $dP/dt$ (Min $dP/dt$) were used as indices of hemodynamics, and recorded simultaneously during ventilation after a minimum equilibration period of 20 min.

### 2.6. Echocardiographic studies

Echocardiography was performed on day 21 post-myosin injection. Rats were anesthetized with an intraperitoneal injection of 20 mg/kg sodium pentobarbital. A 12 MHz probe was placed at the left 4th intercostal space for M-mode imaging using 2D echocardiography (Sonos 5500, Philips, Bothell, WA, USA). Left ventricular systolic dimension (LVDs), left ventricular diastolic dimension (LVDd), anterior wall thickness (AWT), posterior wall thickness (PWT) and ejection fraction (EF) were measured, and taken as an average of three beats. Fractional shortening (%FS) was calculated as $(LVDd-LVDs)/LVDd\times100$.

### 2.7. Histological examination

The heart was excised above the origin of the great vessels, and heart weight and body weight were recorded on day 21 post-myosin injection. Portions of the midventricular heart, spleen, pancreas, kidney and liver were fixed with 4% paraformaldehyde, embedded in paraffin, sectioned at 4-μm thickness, stained with either hematoxylin and eosin (H & E) or Masson's trichrome, and subjected to immunohistochemical staining. H & E-stained sections were evaluated by a cardiovascular pathologist (H.I.-U.) for the characterization of myocardial injury and inflammation without knowledge of the experimental groups, on the following scale: 0, absent or questionable presence; 1, limited focal distribution; 2–3, intermediate severity; and 4, coalescent and extensive foci throughout the entire transversely sectioned ventricular tissue.

### 2.8. Immunohistochemical study

Paraffin-embedded heart sections were washed in increasing concentrations of ethanol and then with PBS. Sections were incubated with Protein Block (DakoCytomation, Glostrup, Denmark), then with mouse anti-rat von Willebrand Factor (vWF) (DakoCytomation), CD68 (DakoCytomation) or monocyte chemoattractant protein-1 (MCP-1) (BD Biosciences Pharmingen, San Jose, CA, USA) antibody in diluent for 40 min, followed by incubation with horseradish peroxidase (HRP)-linked rabbit anti-mouse IgG (DakoCytomation) for 30 min. Sections were visualized using 0.5% diaminobenzidine and 0.03% hydrogen peroxide, and counterstained with hematoxylin. The numbers of CD68-stained cells and vWF-stained capillaries were determined in 10 randomly selected fields (×200).

### 2.9. Enzyme-linked immunosorbent assay (ELISA)

Serum MCP-1 level of rats on day 21 post-myosin injection was measured using a Rat MCP-1 ELISA kit (Biosource International, Carmarillo, CA, USA). Vascular endothelial growth factor (VEGF) and hepatocyte growth factor (HGF) levels in the supernatant of MSC culture ($2.3 \times 10^5$ cells in 10-cm dish cultured for 48 h) were measured using ELISA kits, according to the manufacturers' protocols (HGF, Institute of Immunology, Tokyo, Japan; VEGF, R&D Systems, Minneapolis, MN, USA).

### 2.10. Isolation of cardiomyocytes

Ventricular cardiomyocytes were obtained as described previously with modification [9]. Briefly, after heparinization by intraperitoneal injection of 1000 U/kg heparin sodium, the heart was rapidly excised, and pulmonary, connective and other noncardiac tissues were removed. The heart was then mounted on the cannula of a modified Langendorff apparatus and perfused with buffer containing 0.75 mg/ml collagenase type I (Worthington, Lakewood, NJ, USA), 0.5 mg/ml hyaluronidase (Sigma) and 1% bovine serum albumin (fraction V, ICN, Aurora, OH, USA), in a recirculating fashion for 3 h. After the perfusion sequence, the heart was removed from the perfusion apparatus, the atrium was removed, and gently minced. The enzyme-containing buffer was harvested and the cardiomyocytes resuspended in fresh buffer. The calcium concentration in the suspension was raised stepwise to 1.2 mM. Quiescent, calcium-tolerant cardiomyocytes were gravitationally separated from any nonventricular cells and resuspended in complete culture medium. The culture medium was exchanged for fresh medium to remove the damaged myocytes that failed to attach 3 h after plating. After this procedure, 80% to 90% myocytes were viable and showed rod-shape.

### 2.11. Cardiomyocyte stimulation and MTS assay

To assess cardioprotective effects of MSC acting in a paracrine manner, we investigated whether conditioned medium obtained from MSC culture attenuated MCP-1-induced cardiomyocyte injury. Cardiomyocytes were plated on 96-well plates ($1 \times 10^3$ viable cells/well) precoated with laminin (BD Biosciences Pharmingen). After 3 h, the medium was changed to fresh DMEM containing 15% FBS or conditioned medium obtained from MSC culture, with or without 50 ng/ml MCP-1 (R&D Systems, Minneapolis, MN, USA). After 24 h, the cellular level of 3-(4,5-dimethylthiazol-2-yl)-5-(3-carboxymethoxyphenyl)-2-(4-sulfophenyl)-2H-tetrazolium (MTS), indicative of the mitochondrial function in living cells and cell viability, was measured ($n=6$) with a CellTiter96 AQueous One Kit (Promega, Madison, WI, USA) and a Microplate Reader (490 nm, Bio-Rad, Hercules, CA, USA).

### 2.12. In vitro apoptosis assay

Terminal dUTP nick end labeling (TUNEL) assay (ApopTag Fluorescein In Situ Apoptosis Detection Kit, Chemicon International, Temecula, CA, USA) was performed to evaluate apoptosis of cultured cardiomyocytes. After incubation for 24 h, cardiomyocytes were fixed in 1% paraformaldehyde, and TUNEL staining was performed for detection of apoptotic nuclei according to the manufacturer's

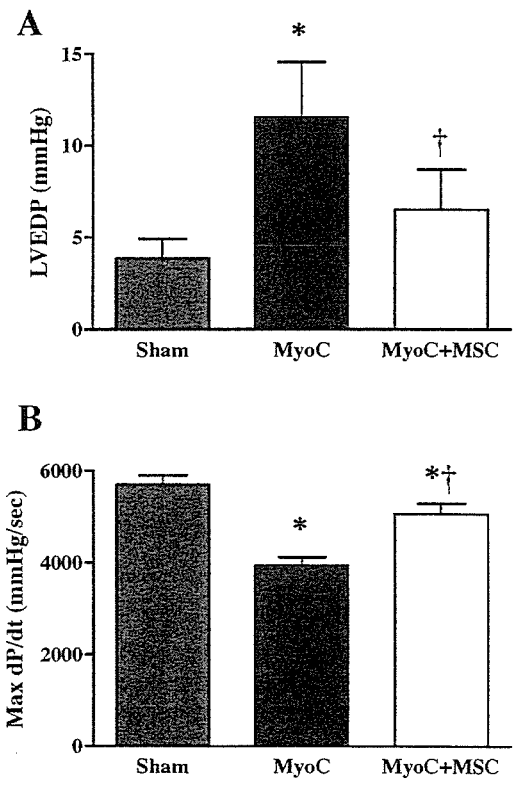


Fig. 1. Effects of MSC transplantation on hemodynamic parameters in acute myocarditis. (A) Left ventricular end-diastolic pressure (LVEDP) and (B) maximum d$P$/d$t$ (Max d$P$/d$t$) were measured in sham-operated rats given vehicle (Sham group), myosin-treated rats given vehicle (MyoC group), and myosin-treated rats given MSC (MyoC+MSC group). Values are mean±S.E. *$P<0.05$ *vs* Sham, †$P<0.05$ *vs* MyoC group.

Table 1
Physiological parameters in three experimental groups

| | Sham | MyoC | MyoC+MSC |
|---|---|---|---|
| HW/BW (g/kg) | 2.9±0.3 | 6.4±0.3* | 4.7±0.3*,† |
| HR (bpm) | 446±11 | 363±14* | 442±12*,† |
| MAP (mm Hg) | 108±3 | 87±3* | 108±4† |
| LVSP (mm Hg) | 130±2 | 105±4* | 125±4† |
| Min d*P*/d*t* (mm Hg/s) | −5440±199 | −3097±183* | −4617±171*,† |

Sham, sham-operated rats given vehicle; MyoC, myosin-treated rats given vehicle; MyoC+MSC, myosin-treated rats given MSC ($3\times10^6$ cells); HW/BW, heart weight to body weight ratio; HR, heart rate; MAP, mean arterial pressure; LVSP, left ventricular systolic pressure; Mim d*P*/d*t*, minimum d*P*/d*t*. Data are mean±S.E. *$P<0.05$ *vs* Sham, †$P<0.05$ *vs* MyoC group.

instructions. The cells were then mounted in medium containing DAPI. Randomly selected microscopic fields ($n=5$) were evaluated to calculate the ratio of TUNEL-positive cells to total cells.

Table 2
Echocardiographic findings in three experimental groups

| | Sham | MyoC | MyoC+MSC |
|---|---|---|---|
| LVDs (mm) | 3.1±0.1 | 5.0±0.4* | 3.8±0.2† |
| EF (%) | 74.9±1.2 | 56.6±3.4* | 71.2±3.5† |
| AWT diastole (mm) | 1.9±0.1 | 3.0±0.2* | 3.0±0.3* |
| PWT diastole (mm) | 1.9±0.1 | 3.4±0.1* | 2.7±0.2*,† |

Sham, sham-operated rats given vehicle; MyoC, myosin-treated rats given vehicle; MyoC+MSC, myosin-treated rats given MSC ($3\times10^6$ cells); LVDs, left ventricular systolic dimension; EF, ejection fraction; AWT, anterior wall thickness; PWT, posterior wall thickness. Data are mean±S.E. *$P<0.05$ *vs* Sham, †$P<0.05$ *vs* MyoC group.

### 2.13. Creatine kinase (CK) activity assay

CK activity in culture media was measured after incubation of cardiomyocytes for 24 h ($n=5$), using the enzyme measurement kit (Kanto Chemical, Tokyo, Japan).

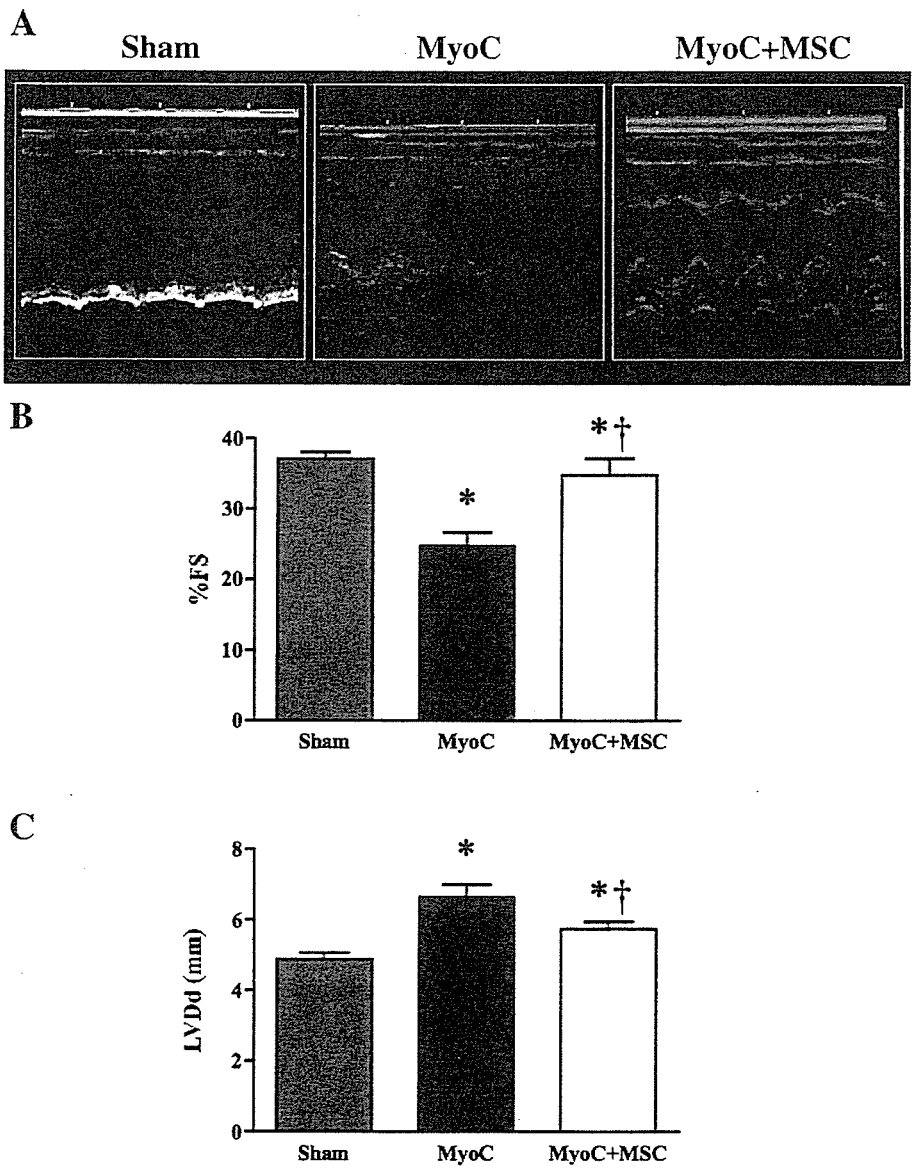


Fig. 2. Effects of MSC transplantation on echocardiographic parameters in acute myocarditis. (A) Representative echocardiographic images showing wall thickening and poor movement in the MyoC group, and improvement of cardiac contractility in the MyoC+MSC group. (B and C) MSC transplantation significantly improved fractional shortening (%FS) and left ventricular diastolic dimension (LVDd). Values are mean±S.E. *$P<0.05$ *vs* Sham, †$P<0.05$ *vs* MyoC group.

### 2.14. Statistical analysis

Data were expressed as mean ± standard error (S.E.). Comparisons of parameters among groups were made by one-way ANOVA, followed by Newman–Keuls' test. Differences were considered significant at $P<0.05$.

## 3. Results

### 3.1. Improvement in cardiac function by MSC transplantation

Two of 15 rats in the MyoC group died on day 19 and day 21 post-myosin injection, respectively, whereas the MyoC+MSC group had no mortality. At 3 weeks post-myosin injection, the MyoC group showed increased heart weight/body weight ratio (HW/BW) and LVEDP, and decreased MAP and Max d*P*/d*t* compared with the Sham group, indicating the presence of acute heart failure in this model (Fig. 1 and Table 1). These parameters subsequently returned to baseline with MSC transplantation (MyoC+MSC group). On echocardiography, the MyoC group showed an increase in LVDs and LVDd, and a significant reduction in %FS and EF (Fig. 2 and Table 2). MSC transplantation significantly improved these parameters (MyoC+MSC group).

### 3.2. Attenuation of myocardial inflammation by MSC transplantation

Myocardial necrosis and tissue granulation as well as giant cell infiltration and edema were markedly increased in our model of acute myocarditis (Fig. 3A). MSC transplantation significantly attenuated these changes observed in the MyoC group. MSC-transplanted hearts exhibited a consistent tendency for a reduction of tissue granulation, inflammation and edema, on blinded histological grading by a cardiovascular pathologist (H.I-U.), as compared to the MyoC group (Fig. 3B). Hearts showed limited fibrosis in the MyoC group, and this observation was not significantly attenuated by MSC

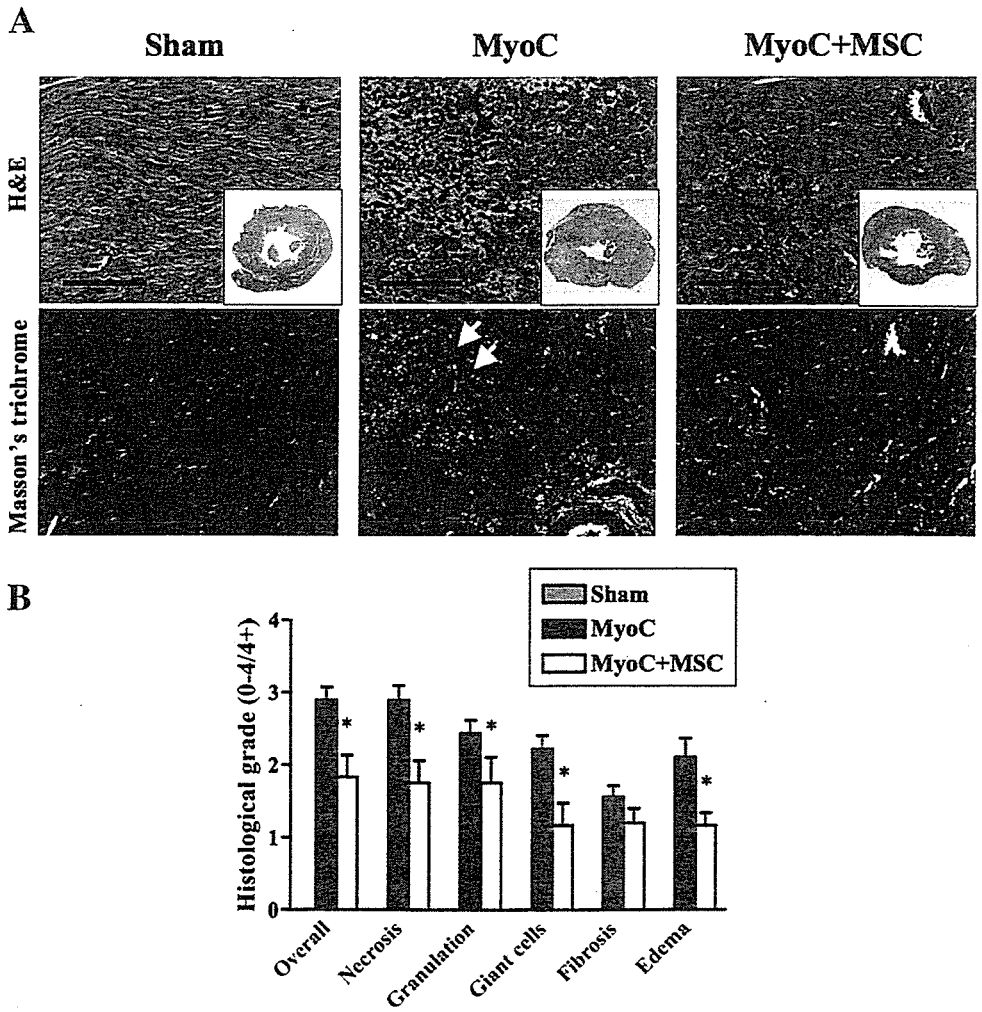


Fig. 3. Effects of MSC transplantation on pathological changes in acute myocarditis. (A) Representative myocardial sections show markedly decreased inflammation and tissue necrosis (H & E) and a comparable degree of early fibrosis (Masson's trichrome) after MSC transplantation (MyoC+MSC) as compared to control (MyoC, arrows). Insets are transverse sections of myocardium. Scale bars: 50 μm. (B) Semi-quantitative histological grades for necrosis and tissue granulation as well as for infiltration of giant cells and edema were significantly lower after MSC transplantation (MyoC+MSC) compared to control (MyoC). Sham tissues exhibited no measurable pathological change. Values are mean±S.E. *$P<0.05$ *vs* Sham, †$P<0.05$ *vs* MyoC group.

transplantation, possibly because of the acute nature of this experiment (Fig. 3B).

Notably, marked histiocytic infiltration was demonstrated by CD68-positive cells, including multinucleated giant cells, in myocarditis (MyoC group), and this was significantly attenuated by MSC transplantation (Figs. 4A and B). In myocarditis, there was an increase in MCP-1 expression localized to the vascular endothelium and also in cardiomyocytes surrounding areas of inflammation (Fig. 5A). The hearts in the MyoC+MSC group showed a partial decrease in MCP-1 expression. Serum MCP-1 level was greatly increased in the MyoC group, whereas the increase was significantly attenuated in the MyoC+MSC group (Fig. 5B).

### 3.3. Effect of MSC on angiogenesis

To investigate the angiogenic effect of MSC transplantation in the myocardium, immunohistochemical analysis of vWF was performed. Capillary density was increased in the MyoC group (Figs. 6A and B). Notably, in MSC-transplanted tissues, capillary density was increased compared to that in the MyoC group. The clustering of relatively small vessels seen in MSC-transplanted hearts was indicative of recent neovascularization.

### 3.4. Cardioprotective effects of MSC in paracrine manner

Because MSC transplantation had anti-inflammatory and tissue-protective effects and induced angiogenesis, some paracrine effects were expected. To confirm the paracrine effects of MSC *in vitro*, cardiomycytes were isolated from adult rats, and cultured with MCP-1 in the standard medium or in the conditioned medium obtained from MSC culture. The standard medium containing MCP-1 resulted in a decrease in viable cardiomyocytes; however, MSC-derived conditioned medium containing MCP-1 attenuated the decrease in viable cardiomyocytes (Fig. 7A). TUNEL staining showed that the standard medium containing MCP-1 markedly induced apoptosis of cardiomyocytes (Figs. 7B and C). However, the conditioned medium of MSC significantly attenuated MCP-1-induced cardiomyocyte apoptosis. In addition, CK activity in standard medium containing MCP-1 was significantly increased, whereas the conditioned medium markedly attenuated the CK activity induced by MCP-1 (Fig. 7D).

To investigate whether MSC secreted angiogenic and anti-fibrotic factors, VEGF and HGF levels in MSC culture were measured by ELISA assay. MSC secreted large amounts of VEGF and HGF compared to standard medium, respectively (Fig. 7E).

## 4. Discussion

In this study, we focused on the therapeutic potential of MSC transplantation in the acute phase of myocarditis. We showed that 1) MSC transplantation 1 week after myosin injection improved cardiac function and attenuated pathological findings including myocardial inflammation, and that 2)

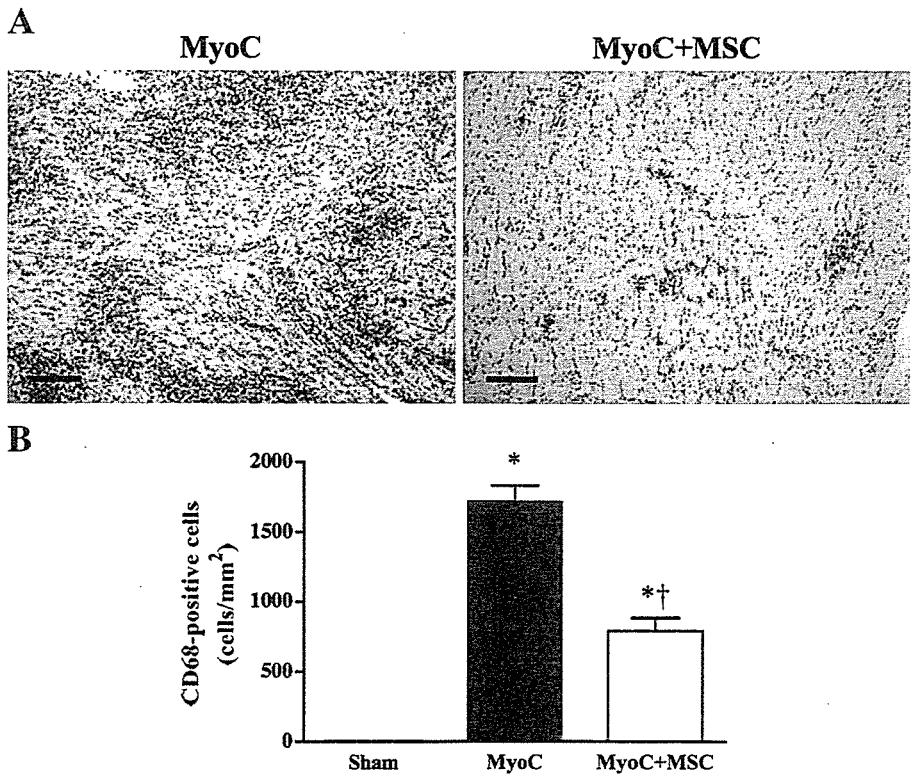


Fig. 4. Effects of MSC transplantation on myocardial CD68 expression in acute myocarditis. (A) Representative myocardial sections immunohistochemically stained for CD68 demonstrate a marked decrease in CD68-positive cells, including giant cells, after MSC transplantation (MyoC+MSC) as compared to control (MyoC). Scale bars: 100 μm. (B) Semi-quantitative counts of CD68-positive cells demonstrate a significant reduction in the MyoC+MSC group. Values are mean±S.E. *$P<0.05$ *vs* Sham, †$P<0.05$ *vs* MyoC group.

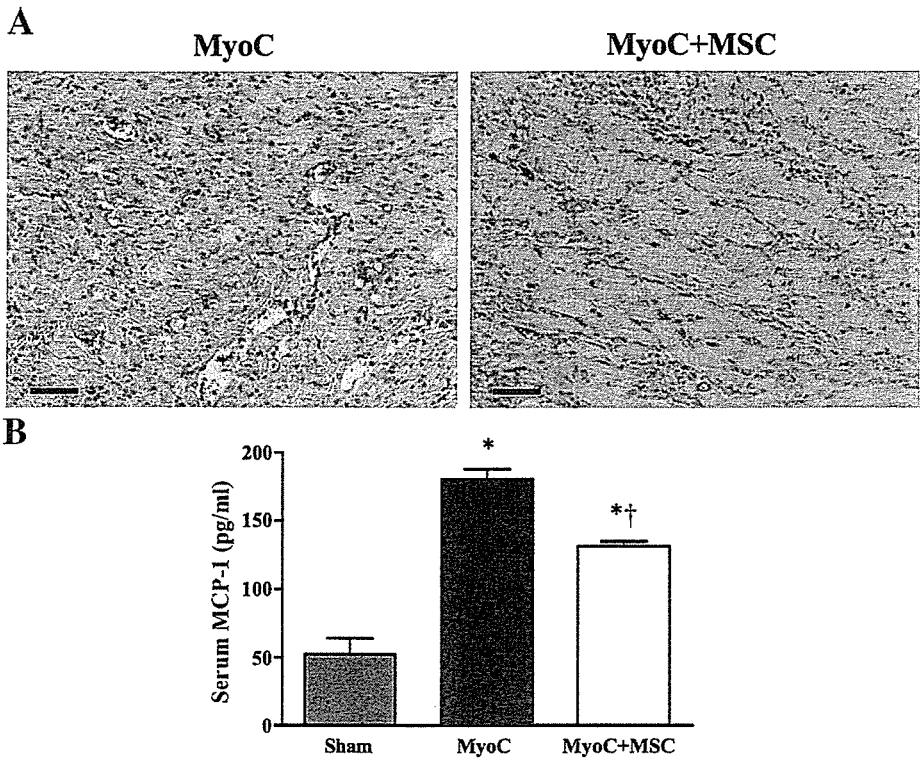


Fig. 5. Effects of MSC transplantation on myocardial MCP-1 expression and serum MCP-1 level. (A) Representative MCP-1-stained myocardial sections from MyoC and MyoC+MSC groups. Scale bars: 50 μm. (B) Serum level of MCP-1 measured by ELISA. Values are mean±S.E. *$P<0.05$ *vs* Sham, †$P<0.05$ *vs* MyoC group.

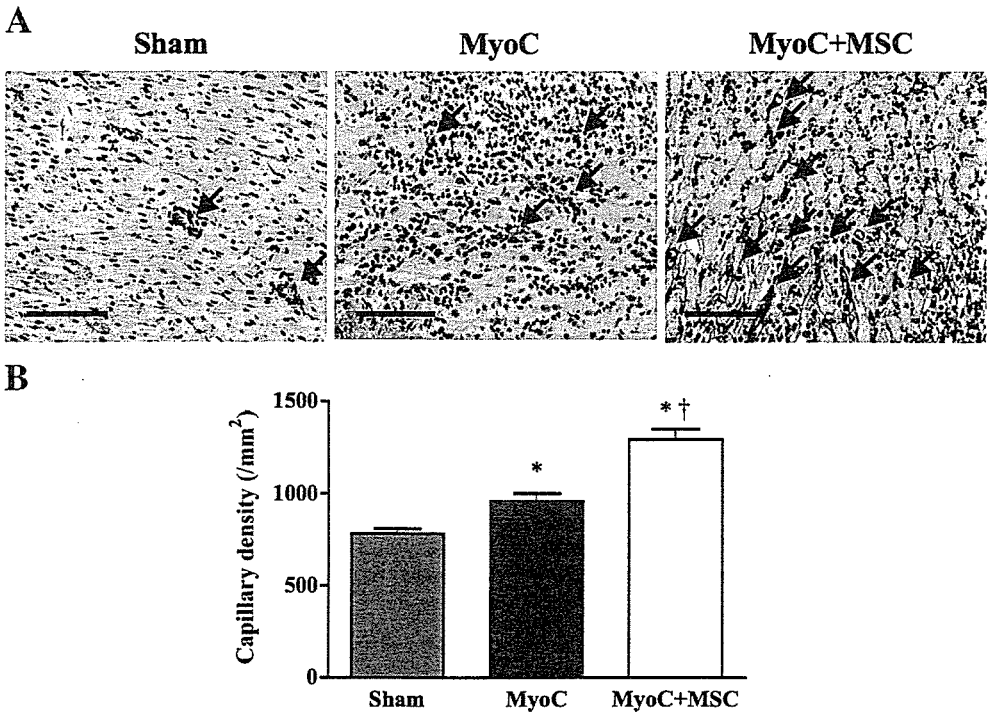


Fig. 6. Effects of MSC on neovascularization. (A) Representative myocardial sections immunohistochemically stained for vWF showing increased microvasculature (arrows) in control hearts (MyoC), which was more marked after MSC transplantation (MyoC+MSC). Scale bars: 50 μm. (B) Capillary density measured in 10 random representative high-power fields showing a significant increase in control (MyoC) and a further increase after MSC transplantation (MyoC+MSC) over the Sham group. Values are mean±S.E. *$P<0.05$ *vs* Sham, †$P<0.05$ *vs* MyoC group.

MSC had cardioprotective effects acting in a paracrine manner.

The rat model of myosin-induced experimental myocarditis provides a model that resembles human giant cell myocarditis [8,10]. Although the majority of acute myocarditis is linked to a viral infection such as coxsackievirus B3, this viral infection can in some cases cause an autoimmune myocarditis with chronic myocardial inflammation without viral persistence, due to the exposure of cardiac autoantigens to the immune system [11,12]. This myocarditis model is triphasic, consisting of an antigen priming phase from days 0–14, an autoimmune response phase from days 14–21, and a reparative phase thereafter, associated chronically with a dilated cardiomyopathy phenotype [13]. In our previous study, MSC were transplanted at the reparative

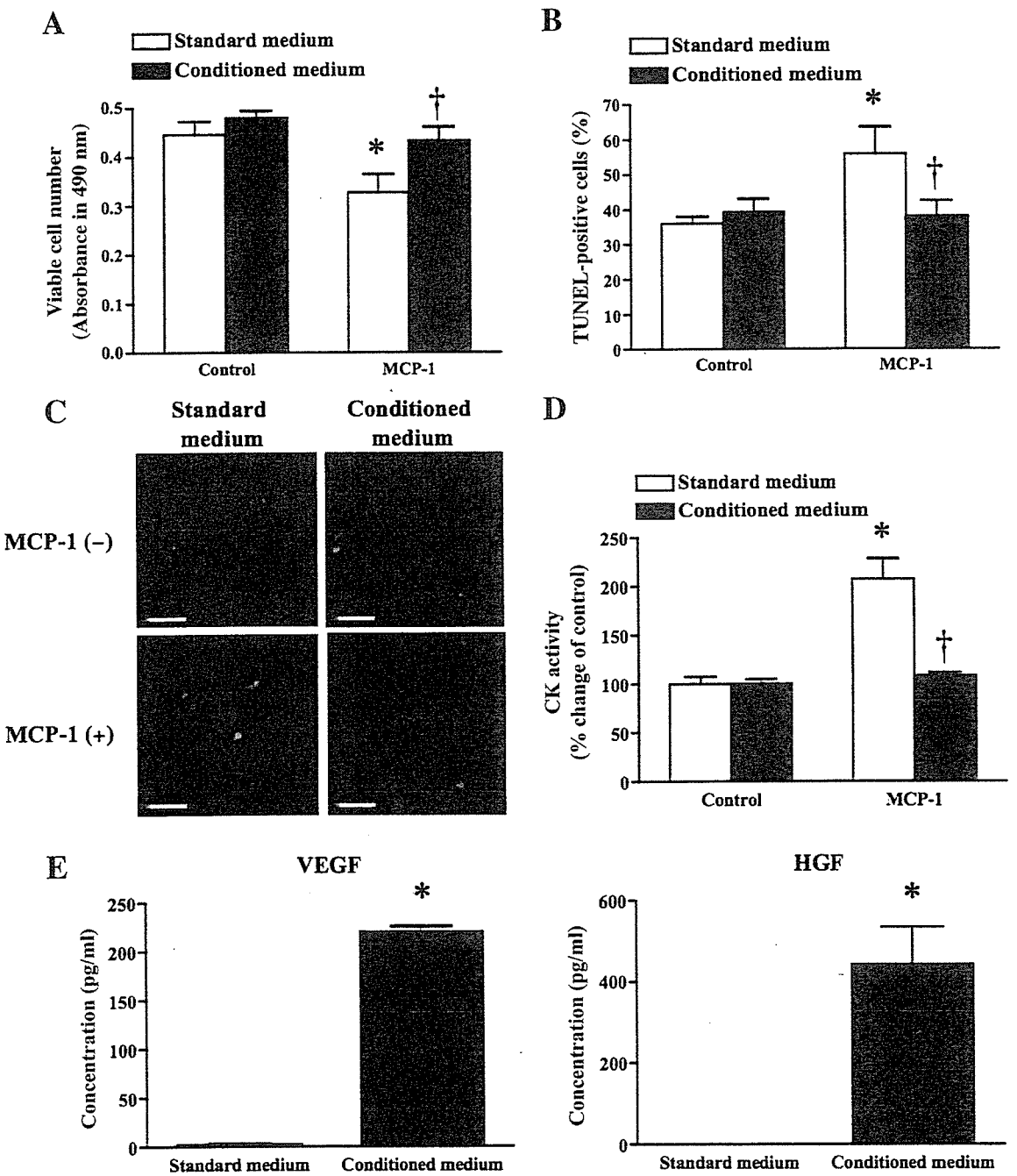


Fig. 7. Effects of MSC on MCP-1-induced cardiomyocyte injury *in vitro*. (A) MTS assay after 24 h of culture with or without MCP-1 in standard medium *vs* MSC conditioned medium. $^{*}P<0.05$ *vs* control in standard medium, $^{\dagger}P<0.05$ *vs* MCP-1 in conditioned medium. (B) Quantitative analysis of TUNEL staining after 24 h of culture with or without MCP-1 in standard medium *vs* MSC conditioned medium. $^{*}P<0.05$ *vs* control in standard medium, $^{\dagger}P<0.05$ *vs* MCP-1 in standard medium. (C) Representative TUNEL staining show increased apoptotic cardiomyocytes (green) cultured with MCP-1 in standard medium, which was attenuated by MSC conditioned medium. Nuclei were counterstained with DAPI (blue). Scale bars: 50 μm. (D) CK activity after 24 h of culture with or without MCP-1 in standard medium *vs* MSC conditioned medium. $^{*}P<0.05$ *vs* control in standard medium, $^{\dagger}P<0.05$ *vs* MCP-1 in standard medium. (E) ELISA for VEGF and HGF secreted from cultured MSC as compared to standard medium. $^{\dagger}P<0.05$ *vs* standard medium.

# Physiological Significance and Therapeutic Potential of Adrenomedullin in Pulmonary Hypertension

Shinsuke Murakami[1,2], Hiroshi Kimura[2], Kenji Kangawa[3] and Noritoshi Nagaya[1,*]

[1]*Department of Regenerative Medicine and Tissue Engineering, National Cardiovascular Center Research Institute, Osaka, Japan,* [2]*Second Department of Internal Medicine, Nara Medical University, Nara, Japan,* [3]*Department of Biochemistry, National Cardiovascular Center Research Institute, Osaka, Japan*

**Abstract:** Adrenomedullin (ADM) is a potent vasodilator peptide that was originally isolated from human pheochromocytoma. Its vasodilatory effect is mediated by cyclic adenosine 3',5'-monophosphate- and nitric oxide-dependent mechanisms. Earlier studies have demonstrated that ADM is secreted from various tissues, including vessels, heart, and lungs. In addition, there are specific receptors for ADM in the lungs. Plasma ADM level is elevated in proportion to the severity of pulmonary hypertension, and circulating ADM is partially metabolized in the lungs. These findings suggest that ADM plays an important role in the regulation of pulmonary vascular tone. Administration of ADM by intravenous or intratracheal delivery significantly decreased pulmonary arterial pressure and pulmonary vascular resistance in patients with pulmonary arterial hypertension. Furthermore, we have recently developed a new therapeutic strategy using ADM gene-modified endothelial progenitor cells (EPC). Intravenously administered ADM gene-modified EPC were incorporated into lung tissues and attenuated monocrotaline-induced pulmonary hypertension in rats. In addition, ADM has angiogenic and anti-apoptotic activities *via* activation of Akt and/or mitogen-activated protein kinase. These findings suggest that ADM may act not only as a vasodilator but also as a vasoprotective factor. Thus, ADM may be a promising endogenous peptide for the treatment of pulmonary hypertension.

**Key Words:** Adrenomedullin, pulmonary hypertension, vasodilation, cyclic adenosine 3',5'-monophosphate, nitric oxide, endothelial progenitor cell, gene therapy, angiogenesis, anti-apoptosis, Akt.

## INTRODUCTION

Idiopathic pulmonary arterial hypertension (IPAH) is a rare but life-threatening disease characterized by increasing pulmonary vascular resistance and progressive pulmonary hypertension that leads to right ventricular failure and death [1]. The median survival is estimated to be 2.8 years from diagnosis [2]. Because the presence of endothelial abnormalities in the pulmonary vascular bed causes pulmonary vasoconstriction, smooth muscle cell proliferation, and *in situ* thrombosis [3], a variety of vasodilators, anti-proliferative agents, and anticoagulants have been proposed as therapeutic agents for IPAH [4-6]. Despite therapeutic medical advances including prostacyclin therapy, some patients ultimately require heart-lung or lung transplantation [7,8]. Thus, a novel therapeutic strategy is desirable for the treatment of pulmonary hypertension.

Adrenomedullin (ADM), which was originally isolated from human pheochromocytoma, is a potent and long-lasting hypotensive peptide [9]. Human ADM consists of 52 amino acids with a single intramolecular disulfide bond and an amidated tyrosine at the carboxy terminus (Fig. **1**) [9]. This peptide shares some structural homology with calcitonin gene-related peptide and amylin. The effects of ADM are mediated by two Gs-protein-coupled plasma membrane receptors: calcitonin-receptor-like receptor and receptor activity-modifying protein-2 or -3 [10]. Subsequent studies

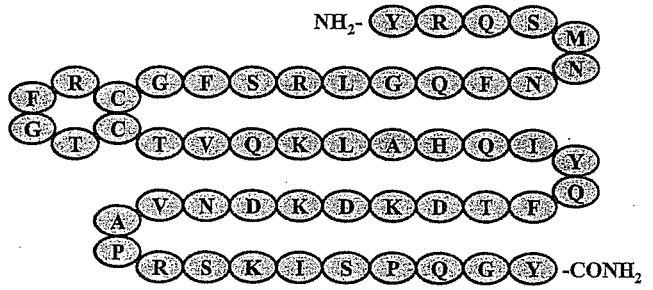


**Fig. (1).** Human adrenomedullin consists of 52 amino acids with a single intramolecular disulfide bond between residues 16 and 21 and with an amidated tyrosine at the carboxy terminus.

have revealed that immunoreactive ADM is distributed in plasma and a wide range of tissues including aorta, ventricles, lungs, and kidneys [11,12]. In particular, ADM is actively produced and secreted by vascular endothelial cells and vascular smooth muscle cells [13-15]. In addition to potent vasodilating effects, ADM has been reported to have multiple effects on cardiovascular and renal function, such as diuretic and natriuretic effects [16,17], and a positive inotropic effect [18,19]. Recently, ADM has received much attention as an important factor in cell growth and survival [20-25]. Thus, ADM has come to be regarded as a multifunctional peptide.

Previous studies have shown that plasma and/or tissue ADM levels are elevated in a variety of cardiovascular and renal diseases including hypertension [26-28], acute myocardial infarction [29-32], heart failure [33-39], and renal failure [40]. We and others have reported that plasma

*Address correspondence to this author at the Department of Regenerative Medicine and Tissue Engineering, National Cardiovascular Center Research Institute, 5-7-1 Fujishirodai, Suita, Osaka 565-8565, Japan; Tel: +81-6-6833-5012; Fax: +81-6-6872-7485; E-mail: nnagaya@ri.ncvc.go.jp

1871-529X/06 $50.00+.00 

ADM levels are also elevated in patients with pulmonary hypertension in proportion to the clinical severity [41-43]. These findings suggest that ADM may be involved in the regulation of cardiovascular and renal function and vascular tone. Recent studies have reported that in heterozygous ADM knockout mice with almost half the level of ADM in organs and plasma, marked cardiac hypertrophy and coronary artery lesions were observed under conditions of high cardiovascular stress [44,45]. Thus, endogenous ADM may possess a protective effect against cardiovascular damage, and increased plasma and/or tissue ADM levels may be a compensatory response to organ failure.

This review summarizes the physiological significance of ADM in patients with pulmonary hypertension and the therapeutic potential of ADM for the treatment of pulmonary hypertension.

## PLASMA LEVELS OF ADRENOMEDULLIN IN PATIENTS WITH PULMONARY HYPERTENSION

Plasma ADM levels have been reported to be elevated in patients with pulmonary arterial hypertension [46] and in animal models of experimental pulmonary hypertension induced by monocrotaline [47]. To investigate the pathophysiological significance of ADM in pulmonary hypertension, we studied the relationship between plasma ADM levels and pulmonary hemodynamics in patients with pulmonary arterial hypertension [41]. Plasma ADM levels in patients with pulmonary arterial hypertension were significantly higher than those in healthy subjects. In addition, there were significant correlations between the plasma ADM level and mean pulmonary arterial pressure, total pulmonary resistance, and mean right arterial pressure. These findings suggest that the plasma ADM level is increased in proportion to the severity of pulmonary hypertension and right heart failure.

Previous studies have shown that ADM mRNA and its receptor mRNA are highly expressed in the lung [48]. Yoshibayashi *et al.* measured plasma ADM levels in blood samples obtained from various sites during cardiac catheterization in patients with pulmonary hypertension [46]. The plasma ADM level in the pulmonary vein was significantly lower than that in the pulmonary artery, consistent with the previous finding that the pulmonary circulation is the site of ADM clearance [49]. These findings suggest that elevated endogenous ADM in plasma may play an important role in the pulmonary circulation.

Previous studies have demonstrated that hypoxia, cytokine production, and shear stress induce ADM secretion by vascular cells [50-52]. An *in vitro* study has demonstrated that ADM is upregulated through a hypoxia-inducible factor-1 (HIF-1)-dependent pathway under hypoxic conditions [53]. Thus, hypoxia/HIF-1 is one of the most potent regulators of ADM production in pulmonary arterial hypertension.

## BIOLOGICAL ACTIONS OF ADRENOMEDULLIN

Intravenous infusion of ADM results in potent and sustained hypotension [17,44,54,55]. ADM has been shown to increase the intracellular cyclic adenosine 3',5'-monophosphate (cAMP) level in vascular smooth muscle cells *via* its specific receptor [56,57]. The increase in cAMP by ADM activates protein kinase A (PKA), resulting in a decrease in calcium content in smooth muscle cells. On the other hand, ADM has been shown to induce vasorelaxation in a nitric oxide (NO)-dependent manner [58]. ADM induces activation of endothelial NO synthase in vascular endothelial cells *via* the $Ca^{2+}$/calmodulin-dependent [59] and the phosphatidylinositol 3-kinase (PI3K)/Akt-dependent pathway [60]. Thus, ADM regulates vascular tone through a cAMP-dependent mechanism and/or a NO-dependent mechanism (Fig. 2). It has been reported that there are many binding sites for ADM in the lung [61] and that ADM preferentially dilates pulmonary arterial resistance vessels [62]. These findings raise the possibility that ADM may play an important role in the regulation of pulmonary vascular tone in patients with pulmonary hypertension.

An imbalance between vasodilators and vasoconstrictors has been thought to have a key role in the development of IPAH [63]. Endothelial dysfunction decreases the production of vasodilators such as prostacyclin and NO, whereas it increases that of vasoconstrictors including thromboxane and endothelin-1 [3]. Previous studies demonstrated that prostacyclin synthase [64] and endothelial nitric oxide synthase [65] expression were decreased in the lungs of patients with pulmonary hypertension. Thus, pulmonary endothelial cells may be a therapeutic target for the treatment of pulmonary hypertension. ADM regulates growth and survival of endothelial cells [22,66,67]. ADM signaling is of particular significance in endothelial biology, since the peptide protects cells from apoptosis and promotes angiogenesis at least in part through activation of PI3K/Akt and mitogen-activated protein kinase/extracellular signal-regulated kinase 1/2 in endothelial cells. These findings raise the possibility that elevated plasma ADM in patients with pulmonary hypertension may exert protective effects on pulmonary endothelial cells.

Plexiform lesions, the classic pathological finding in IPAH, are present in about one in three lung biopsy specimens [68]. These lesions have been considered an abnormal growth of modified smooth muscle cells [69]. *In vitro*, ADM has been shown to inhibit serum or platelet-derived growth factor-stimulated proliferation and migration in smooth muscle cells [70-72]. *In vivo*, continuous infusion of ADM has been shown to inhibit pulmonary smooth muscle cell proliferation in monocrotaline-induced pulmonary hypertension in rats [73]. These results suggest that ADM may have an inhibitory function in pulmonary vascular remodeling.

The overproduction of reactive oxygen species results in the progression of pulmonary vascular remodeling. ADM is recognized as a potent antioxidant. An *in vitro* study showed ADM suppressed reactive oxygen species production in a dose-dependent manner *via* activation of the cAMP-protein kinase A pathway [74]. Heterozygous ADM knockout mice housed under hypoxia showed not only severe pulmonary vascular injury but also higher levels of reactive oxygen species production [75]. These findings suggest that ADM might be one of the important compensatory substances to protect against hypoxia-induced pulmonary vascular remodeling, possibly through the suppression of reactive oxygen species.

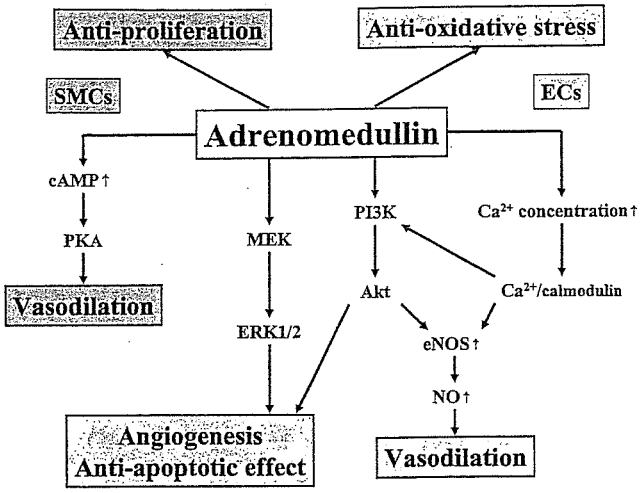


**Fig. (2).** Signaling pathway of adrenomedullin (ADM) in vascular endothelial cells (ECs) and smooth muscle cells (SMCs). ADM regulates vascular tone through a cAMP-dependent mechanism and/or a NO-dependent mechanism. ADM protects cells from apoptosis and promotes angiogenesis at least in part through activation of Akt and ERK1/2 in endothelial cells. ADM also inhibits smooth muscle cell proliferation and suppresses reactive oxygen species production.

## THERAPEUTIC POTENTIAL OF ADRENOMEDULLIN IN PULMONARY HYPERTENSION

Previous experimental studies have shown that exogenously administered ADM causes a dose-related decrease in pulmonary arterial pressure under conditions of high pulmonary vascular tone [62,76,77]. Short-term infusion of ADM attenuates pulmonary hypertension secondary to congestive heart failure [78,79], and long-term infusion of ADM attenuates progressive pulmonary hypertension and medial thickening of the pulmonary arteries in rats treated with monocrotaline [73]. However, in humans, it remains unknown whether exogenous ADM has beneficial effects in patients with precapillary pulmonary hypertension such as IPAH or chronic thromboembolic pulmonary hypertension. Accordingly, we examined the hemodynamic and hormonal responses to intravenous infusion of ADM or placebo in 13 patients with precapillary pulmonary hypertension [80]. ADM (0.05μg/kg/minute) or placebo was randomly administered at a rate of 0.5 ml/minute for 30 minutes. At the end of ADM infusion, plasma ADM level was increased about 3-fold in the ADM group. ADM infusion produced a 44% increase in cardiac index and a 32% decrease in pulmonary vascular resistance, and its hemodynamic effects lasted at least 15 minutes after the end of infusion. These results suggest that ADM has potent, relatively long-lasting pulmonary vasodilator activity in patients with pulmonary hypertension. We have shown that plasma cAMP level was increased by 23% during ADM infusion. The increase in cAMP by ADM activates PKA, resulting in a decrease in calcium content in smooth muscle cells [57]. It is therefore possible that ADM may relax vascular smooth muscle by inducing an increase in cAMP level. ADM infusion markedly increased the cardiac index in patients with pulmonary hypertension. Considering the strong vasodilator activity of ADM in the systemic and pulmonary vasculature, a significant decrease in cardiac afterload may be responsible for the increased cardiac index with ADM. On the other hand, a previous binding study has shown abundant, specific binding sites for ADM in ventricular myocardium [61]. ADM has been shown to increase cardiac cAMP [81,82], which is known to mediate the positive inotropic action of beta-adrenergic stimulation. Alternatively, ADM has been shown to produce a positive inotropic action through cAMP-independent mechanisms [83]. These findings suggest that the increase in cardiac index may be attributable not only to a fall in cardiac afterload but also to the direct positive inotropic action of ADM. Further studies are necessary to investigate the therapeutic potential and safety of ADM in patients with pulmonary hypertension.

Intravenously administered ADM decreased systemic vascular resistance and induced systemic hypotension in patients with pulmonary hypertension because of nonselective vasodilation in the pulmonary and systemic vascular beds. Recently, inhalation of aerosolized prostacyclin and its analogue, iloprost, has been shown to cause pulmonary vasodilation without systemic hypotension in patients with IPAH [84,85]. In addition, inhalant application of vasodilators does not impair gas exchange because the ventilation-matched deposition of drug in the alveoli causes pulmonary vasodilation matched to ventilated areas. In clinical settings, inhalation therapy may be more simple, noninvasive, and comfortable than continuous intravenous infusion therapy. These findings raise the possibility that ADM inhalation may have beneficial effects in patients with precapillary pulmonary hypertension. We examined the effects of ADM inhalation on monocrotaline-induced pulmonary hypertension in rats [86]. ADM (5 μg/kg) or saline was inhaled as an aerosol using an ultrasonic nebulizer. To assess the acute effect of inhaled ADM, hemodynamic studies were carried out at 3 weeks after monocrotaline injection. Expectedly, a single 30-minute inhalation of ADM significantly decreased total pulmonary vascular resistance without a significant decrease in mean arterial pressure in rats given monocrotaline. These hemodynamic effects of ADM lasted at least 60

minutes after the end of inhalation. Furthermore, to assess the chronic effect of inhaled ADM, 30-minute inhalation of ADM or saline was repeated four times a day for 3 weeks after monocrotaline injection. Repeated inhalation of ADM markedly decreased mean pulmonary arterial pressure and total pulmonary vascular resistance without systemic hypotension in rats given monocrotaline. Interestingly, repeated inhalation of ADM significantly attenuated an increase in medial wall thickness of peripheral pulmonary arteries and improved survival. Considering the potent vasoprotective effects of ADM such as vasodilation and inhibition of smooth muscle cell migration and proliferation, it is interesting to speculate that ADM trapped in the bronchial epithelium or alveoli leaks to the pulmonary arteries to maintain pulmonary vascular integrity in rats given monocrotaline. von der Hardt *et al.* have reported that aerosolized ADM (6 μg/kg) resulted in a sustained reduction in mean pulmonary arterial pressure in a surfactant-depleted piglet model [87]. There was no significant difference in mean systemic arterial pressure after ADM inhalation. Interestingly, they reported that aerosolized ADM reduced endothelin (ET)-1 mRNA in lung tissue and ET-1 protein expression in pulmonary arteries. ET-1 is a potent pulmonary vasoconstrictor [88] and plays an important role in pulmonary hypertension [89-93]. Thus, reduction of ET-1 expression may contribute to the effect of aerosolized ADM on pulmonary hypertension. Recently, we have investigated the effects of ADM inhalation on pulmonary hemodynamics and exercise capacity in patients with IPAH [94]. Inhalation of aerosolized ADM (10 μg/kg) produced a 22% decrease in pulmonary vascular resistance. However, neither systemic arterial pressure nor heart rate was altered. These results suggest that inhaled ADM improves hemodynamics with pulmonary selectivity. In addition, inhalation of ADM improved exercise capacity, as indicated by increased peak oxygen consumption during exercise. Although further studies are necessary to maximize the efficiency and reproducibility of pulmonary ADM delivery, inhalation of ADM may be a promising approach to treat pulmonary hypertension without affecting the systemic circulation.

Recently, stem or progenitor cell transplantation has received much attention as a novel therapeutic option to regenerate a variety of tissues. In 1997, Asahara *et al.* isolated endothelial progenitor cells (EPC) from human peripheral blood [95]. EPC are mobilized from bone marrow into the peripheral blood in response to tissue ischemia or traumatic injury, migrate to sites of injured endothelium, and differentiate into mature endothelial cells *in situ* [96-98]. Transplantation of EPC has been shown to induce therapeutic angiogenesis in the ischemic heart or limb [99-101]. We have shown that intravenously administered EPC are incorporated into the pulmonary vasculature and attenuate pulmonary hypertension in the rat monocrotaline model of IPAH [102]. Thus, the regeneration of pulmonary vascular endothelium by cell transplantation may be a new therapeutic strategy for the treatment of pulmonary hypertension. A recent study has reported that human telomerase reverse transcriptase gene transfer enhances the angiogenic properties of EPC [103]. Considering the variety of protective effects of ADM on vascular endothelial cells, we hypothesized that ADM gene transfer into EPC may strengthen their therapeutic potential. Recently, Fukunaka *et al.* have developed a nonviral vector, gelatin hydrogel [104,105]. Positively charged gelatin can hold negatively charged plasmid DNA in its lattice structure. DNA-gelatin complexes can delay gene degradation, leading to efficient gene transfer [106,107]. Interestingly, EPC phagocytose ionically linked DNA-gelatin complexes in coculture, which allows nonviral gene transfer into EPC with high efficiency. ADM gene transfer into EPC inhibits cell apoptosis and induces proliferation and migration, suggesting that ADM gene transfer strengthens the therapeutic potential of EPC. Furthermore, genetically modified EPCs markedly secreted ADM peptide and ADM overproduction lasted for more than 16 days. Therefore, transplanted EPC may serve not only as a tissue-engineering tool to reconstruct the pulmonary vasculature but also as a vehicle for gene delivery to injured pulmonary endothelium. We have investigated whether cell (EPC)-based ADM gene transfer causes further improvement in monocrotaline-induced pulmonary hypertension in rats [102]. ADM gene-modified EPC were similarly incorporated into the pulmonary vasculature, and significantly decreased pulmonary vascular resistance compared with EPC alone. A single transplantation of ADM gene-modified EPC improved survival in monocrotaline rats compared with transplantation of EPC alone. Thus, a novel hybrid cell-gene therapy may be a new therapeutic strategy for the treatment of pulmonary hypertension including IPAH. However, the initial success of gelatin-mediated ADM gene therapy reported here should be confirmed by long-term experiments, and extensive toxicity studies in animals are needed before clinical trials.

## SUMMARY

This article describes the physiological significance of ADM and its therapeutic potential for the treatment of pulmonary hypertension. ADM has been shown to possess a variety of actions, including vasodilatory actions, regulation of cell growth and survival, and modulation of hormone secretion. Plasma ADM levels are elevated in patients with pulmonary hypertension in proportion to the clinical severity, and circulating ADM is partially metabolized in the lungs. Nevertheless, exogenously administered ADM induces hemodynamic improvement. These findings suggest that ADM may be a promising therapeutic agent for the treatment of pulmonary hypertension including IPAH. Further studies are necessary to evaluate the long-term efficacy and safety of ADM in patients with pulmonary hypertension.

## ABBREVIATIONS

ADM = Adrenomedullin

cAMP = Cyclic adenosine 3',5'-monophosphate

EPC = Endothelial progenitor cell

ET = Endothelin

IPAH = Idiopathic pulmonary arterial hypertension

NO = Nitric oxide

PI3K = Phosphatidylinositol 3-kinase

PKA = Protein kinase A

## REFERENCES


[1] Rich, S., Dantzker, D.R., Ayres, S.M., Bergofsky, E.H., Brundage, B.H., Detre, K.M., Fishman, A.P., Goldring, R.M., Groves, B.M., Koerner, S.K. Primary pulmonary hypertension. A national prospective study. *Ann. Intern. Med.*, **1987**, *107*, 216-223.

[2] D'Alonzo, G.E., Barst, R.J., Ayres, S.M., Bergofsky, E.H., Brundage, B.H., Detre, K.M., Fishman, A.P., Goldring, R.M., Groves, B.M., Kernis, J.T. Survival in patients with primary pulmonary hypertension. Results from a national prospective registry. *Ann. Intern. Med.*, **1991**, *115*, 343-349.

[3] Archer, S., Rich, S. Primary pulmonary hypertension: a vascular biology and translational research "Work in progress". *Circulation*, **2000**, *102*, 2781-2791.

[4] Barst, R.J., Rubin, L.J., Long, W.A, McGoon, M.D., Rich, S., Badesch, D.B., Groves, B.M., Tapson, V.F., Bourge, R.C., Brundage, B.H. A comparison of continuous intravenous epoprostenol (prostacyclin) with conventional therapy for primary pulmonary hypertension. The Primary Pulmonary Hypertension Study Group. *N. Engl. J. Med.*, **1996**, *334*, 296-302.

[5] McLaughlin, V.V., Genthner, D.E., Panella, M.M., Rich, S. Reduction in pulmonary vascular resistance with long-term epoprostenol (prostacyclin) therapy in primary pulmonary hypertension. *N. Engl. J. Med.*, **1998**, *338*, 273-277.

[6] Rubin, L.J., Mendoza, J., Hood, M., McGoon, M., Barst, R., Williams, W.B., Diehl, J.H., Crow, J., Long, W. Treatment of primary pulmonary hypertension with continuous intravenous prostacyclin (epoprostenol). Results of a randomized trial. *Ann. Intern. Med.*, **1990**, *112*, 485-491.

[7] Reitz, B.A., Wallwork, J.L., Hunt, S.A., Pennock, J.L., Billingham, M.E., Oyer, P.E., Stinson, E.B., Shumway, N.E. Heart-lung transplantation: successful therapy for patients with pulmonary vascular disease. *N. Engl. J. Med.*, **1982**, *306*, 57-64.

[8] Pasque, M.K., Trulock, E.P., Kaiser, L.R, Cooper, J.D. Single-lung transplantation for pulmonary hypertension. Three-month hemodynamic follow-up. *Circulation*, **1991**, *84*, 2275-2279.

[9] Kitamura, K., Kangawa, K., Kawamoto, M., Ichiki, Y., Nakamura, S., Matsuo, H., Eto, T. Adrenomedullin: a novel hypotensive peptide isolated from human pheochromocytoma. *Biochem. Biophys. Res. Commun.*, **1993**, *192*, 553-560.

[10] McLatchie, L.M., Fraser, N.J., Main, M.J., Wise, A., Brown, J., Thompson, N., Solari, R., Lee, M.G., Foord, S.M. RAMPs regulate the transport and ligand specificity of the calcitonin-receptor-like receptor. *Nature*, **1998**, *393*, 333-339.

[11] Ichiki, Y., Kitamura, K., Kangawa, K., Kawamoto, M., Matsuo, H., Eto, T. Distribution and characterization of immunoreactive adrenomedullin in human tissue and plasma. *FEBS Lett.*, **1994**, *338*, 6-10.

[12] Sakata, J., Shimokubo, T., Kitamura, K., Nishizono, M., Iehiki, Y., Kangawa, K., Matsuo, H., Eto, T. Distribution and characterization of immunoreactive rat adrenomedullin in tissue and plasma. *FEBS Lett.*, **1994**, *352*, 105-108.

[13] Shimekake, Y., Nagata, K., Ohta, S., Kambayashi, Y., Teraoka, H., Kitamura, K., Eto, T., Kangawa, K., Matsuo, H. Adrenomedullin stimulates two signal transduction pathways, cAMP accumulation and $Ca^{2+}$ mobilization, in bovine aortic endothelial cells. *J. Biol. Chem.*, **1995**, *270*, 4412-4417.

[14] Sugo, S., Minamino, N., Kangawa, K., Miyamoto, K., Kitamura, K., Sakata, J., Eto, T., Matsuo, H. Endothelial cells actively synthesize and secrete adrenomedullin. *Biochem Biophys. Res. Commun.*, **1994**, *201*, 1160-1166.

[15] Sugo, S., Minamino, N., Shoji, H., Kangawa, K., Kitamura, K., Eto, T., Matsuo, H. Production and secretion of adrenomedullin from vascular smooth muscle cells: augmented production by tumor necrosis factor-alpha. *Biochem. Biophys. Res. Commun.*, **1994**, *203*, 719-726.

[16] Majid, D.S., Kadowitz, P.J., Coy, D.H., Navar, L.G. Renal responses to intra-arterial administration of adrenomedullin in dogs. *Am .J .Physiol.*, **1996**, *270*, F200-F205.

[17] Parkes, D.G., May, C.N. Direct cardiac and vascular actions of adrenomedullin in conscious sheep. *Br. J. Pharmacol.*, **1997**, *120*, 1179-1185.

[18] Szokodi, I., Kinnunen, P., Tavi, P., Weckstrom, M., Toth, M., Ruskoaho, H. Evidence for cAMP-independent mechanisms mediating the effects of adrenomedullin, a new inotropic peptide. *Circulation*, **1998**, *97*, 1062-70.

[19] Nagaya, N., Goto, Y., Satoh, T., Sumida, H., Kojima, S., Miyatake, K., Kangawa, K. Intravenous adrenomedullin in myocardial function and energy metabolism in patients after myocardial infarction. *J. Cardiovasc. Pharmacol.*, **2002**, *39*, 754-760.

[20] Kato, H., Shichiri, M., Marumo, F., Hirata, Y. Adrenomedullin as an autocrine/paracrine apoptosis survival factor for rat endothelial cells. *Endocrinology*, **1997**, *138*, 2615-2620.

[21] Nagaya, N., Mori, H., Murakami, S., Kangawa, K., Kitamura, S. Adrenomedullin: angiogenesis and gene therapy. *Am. J. Physiol. Regul. Integr. Comp .Physiol.*, (in press).

[22] Hanabusa, K., Nagaya, N., Iwase, T., Itoh, T., Murakami, S., Shimizu, Y., Taki, W., Miyatake, K., Kangawa, K. Adrenomedullin enhances therapeutic potency of mesenchymal stem cells after experimental stroke in rats. *Stroke*. **2005**, *36*, 853-858.

[23] Iwase, T., Nagaya, N., Fujii, T., Itoh, T., Ishibashi-Ueda, H., Yamagishi, M., Miyatake, K., Matsumoto, T., Kitamura, S., Kangawa, K. Adrenomedullin enhances angiogenic potency of bone marrow transplantation in a rat model of hindlimb ischemia. *Circulation*, **2005**, *111*, 356-362.

[24] Fujii, T., Nagaya, N., Iwase, T., Murakami, S., Miyahara, Y., Nishigami, K., Ishibashi-Ueda H., Shirai, M., Itoh, T., Ishino, K., Sano, S., Kangawa, K., Mori, H. Adrenomedullin enhances therapeutic potency of bone marrow transplantation for myocardial infarction in rats. *Am. J. Physiol. Heart. Circ. Physiol.*, **2005**, *288*, H1444-H1450.

[25] Okumura, H., Nagaya, N., Itoh, T., Okano, I., Hino, J., Mori, K., Tsukamoto, Y., Ishibashi-Ueda, H., Miwa, S., Tambara, K., Toyokuni, S., Yutani, C., Kangawa, K. Adrenomedullin infusion attenuates myocardial ischemia/reperfusion injury through the phosphatidylinositol 3-kinase/Akt-dependent pathway. *Circulation*, **2004**, *109*, 242-248.

[26] Kohno, M., Hanehira, T., Kano, H., Horio, T., Yokokawa, K., Ikeda, M., Minami, M., Yasunari, K., Yoshikawa, J. Plasma adrenomedullin concentrations in essential hypertension. *Hypertension*, **1996**, *27*, 102-107.

[27] Nishikimi, T., Yoshihara, F., Kanazawa, A., Okano, I., Horio, T., Nagaya, N., Yutani, C., Matsuo, H., Matsuoka, H., Kangawa, K. Role of increased circulating and renal adrenomedullin in rats with malignant hypertension. *Am. J. Physiol. Regul. Integr. Comp. Physiol.*; **2001**, *281*, R2079-R2087.

[28] Nishikimi, T., Horio, T., Kohmoto, Y., Yoshihara, F., Nagaya, N., Inenaga, T., Saito, M., Teranishi, M., Nakamura, M., Ohrui, M., Kawano, Y., Matsuo, H., Ishimitsu, T., Takishita, S., Matsuoka, H., Kangawa, K. Molecular forms of plasma and urinary adrenomedullin in normal, essential hypertension and chronic renal failure. *J. Hypertens.*, **2001**, *19*, 765-773.

[29] Kobayashi, K., Kitamura, K., Hirayama, N., Date, H., Kashiwagi, T., Ikushima, I., Hanada, Y., Nagatomo, Y., Takenaga, M., Ishikawa, T., Imamura, T., Koiwaya, Y., Eto, T. Increased plasma adrenomedullin in acute myocardial infarction. *Am .Heart J.*, **1996**, *131*, 676-680.

[30] Miyao, Y., Nishikimi, T., Goto, Y., Miyazaki, S., Daikoku, S., Morii, I., Matsumoto, T., Takishita, S., Miyata, A., Matsuo, H., Kangawa, K., Nonogi, H. Increased plasma adrenomedullin levels in patients with acute myocardial infarction in proportion to the clinical severity. *Heart*, **1998**, *79*, 39-44.

[31] Nagaya, N., Nishikimi, T., Yoshihara, F., Horio, T., Morimoto, A., Kangawa, K. Cardiac adrenomedullin gene expression and peptide accumulation after acute myocardial infarction in rats. *Am. J. Physiol. Regul. Integr. Comp. Physiol.*, **2000**, *278*, R1019-R1026.

[32] Nagaya, N., Nishikimi, T., Uematsu, M., Yoshitomi, Y., Miyao, Y., Miyazaki, S., Goto, Y., Kojima, S., Kuramochi, M., Matsuo, H., Kangawa, K., Nonogi, H. Plasma adrenomedullin as an indicator of prognosis after acute myocardial infarction. *Heart*, **1999**, *81*, 483-487.

[33] Jougasaki, M., Wei, C.M., McKinley, L.J., Burnett, J.C.Jr., Elevation of circulating and ventricular adrenomedullin in human congestive heart failure. *Circulation*, **1995**, *92*, 286-289.

[34] Nishikimi, T., Saito, Y., Kitamura, K., Ishimitsu, T., Eto, T., Kangawa, K., Matsuo, H., Omae, T., Matsuoka, H. Increased plasma levels of adrenomedullin in patients with heart failure. *J. Am. Coll .Cardiol.*, **1995**, *26*, 1424-1431.

[35] Watanabe, K., Nishikimi, T., Takamuro, M., Yasuda, K., Ishikawa, Y., Tanabe, S., Yamada, O., Nagaya, N., Matsuoka, H., Kangawa, K., Echigo, S. Two molecular forms of adrenomedullin in congenital heart disease. *Pediatr. Cardiol.*, **2003**, *24*, 559-565.

[36] Tambara, K., Fujita, M., Nagaya, N., Miyamoto, S., Iwakura, A., Doi, K., Sakaguchi, G., Nishimura, K., Kangawa, K., Komeda, M. Increased pericardial fluid concentrations of the mature form of adrenomedullin in patients with cardiac remodelling. *Heart,* **2002**, *87*, 242-246.

[37] Yoshihara, F., Nishikimi, T., Horio, T., Yutani, C., Nagaya ,N., Matsuo, H., Ohe, T., Kangawa, K. Ventricular adrenomedullin concentration is a sensitive biochemical marker for volume and pressure overload in rats. *Am. J. Physiol. Heart. Circ. Physiol.*, **2000**, *278*, H633-H642.

[38] Morimoto, A., Nishikimi, T., Yoshihara, F., Horio, T., Nagaya, N., Matsuo, H., Dohi, K., Kangawa, K. Ventricular adrenomedullin levels correlate with the extent of cardiac hypertrophy in rats. *Hypertension,* **1999**, *33*, 1146-1152.

[39] Nagaya, N., Nishikimi, T., Horio, T., Yoshihara, F., Kanazawa, A., Matsuo, H., Kangawa, K. Cardiovascular and renal effects of adrenomedullin in rats with heart failure. *Am. J. Physiol.*, **1999**, *276*, R213-R218.

[40] Ishimitsu, T., Nishikimi, T., Saito, Y., Kitamura, K., Eto, T., Kangawa, K., Matsuo, H., Omae, T., Matsuoka, H. Plasma levels of adrenomedullin, a newly identified hypotensive peptide, in patients with hypertension and renal failure. *J. Clin. Invest.*, **1994**, *94*, 2158-2161.

[41] Kakishita, M., Nishikimi, T., Okano, Y., Satoh, T., Kyotani, S., Nagaya, N., Fukushima, K., Nakanishi, N., Takishita, S., Miyata, A., Kangawa, K., Matsuo, H., Kunieda, T. Increased plasma levels of adrenomedullin in patients with pulmonary hypertension. *Clin. Sci., (Lond)* **1999**, *96*, 33-39.

[42] Vijay, P., Szekely, L., Sharp, T.G., Miller, A., Bando, K., Brown, J.W. Adrenomedullin in patients at high risk for pulmonary hypertension. *Ann. Thorac. Surg.*, **1998**, *66*, 500-505.

[43] Nishikimi, T., Nagata, S., Sasaki, T., Yoshihara, F., Nagaya, N., Horio, T., Matsuo, H., Matsuoka, H., Kangawa, K. The active molecular form of plasma adrenomedullin is extracted in the pulmonary circulation in patients with mitral stenosis: possible role of adrenomedullin in pulmonary hypertension. *Clin. Sci (Lond).*, **2001**, *100*, 61-66.

[44] Shimosawa, T., Shibagaki, Y., Ishibashi, K., Kitamura, K., Kangawa, K., Kato, S., Ando, K., Fujita, T. Adrenomedullin, an endogenous peptide, counteracts cardiovascular damage. *Circulation,* **2002**, *105*, 106-111.

[45] Niu, P., Shindo, T., Iwata, H., Iimuro, S., Takeda, N., Zhang, Y., Ebihara, A., Suematsu, Y., Kangawa, K., Hirata, Y., Nagai, R. Protective effects of endogenous adrenomedullin on cardiac hypertrophy, fibrosis, and renal damage. *Circulation,* **2004**, *109*, 1789-1794.

[46] Yoshibayashi, M., Kamiya, T., Kitamura, K., Saito, Y., Kangawa, K., Nishikimi, T., Matsuoka, H., Eto, T., Matsuo, H. Plasma levels of adrenomedullin in primary and secondary pulmonary hypertension in patients <20 years of age. *Am. J. Cardiol.*, **1997**, *79*, 1556-1558.

[47] Shimokubo, T., Sakata, J., Kitamura, K., Kangawa, K., Matsuo, H., Eto, T. Augmented adrenomedullin concentrations in right ventricle and plasma of experimental pulmonary hypertension. *Life Sci.*, **1995**, *57*, 1771-1779.

[48] Kitamura, K., Sakata, J., Kangawa, K., Kojima, M., Matsuo, H., Eto, T. Cloning and characterization of cDNA encoding a precursor for human adrenomedullin. *Biochem. Biophys. Res. Commun.*, **1993**, *194*, 720-725.

[49] Nishikimi, T., Kitamura, K., Saito, Y., Shimada, K., Ishimitsu, T., Takamiya, M., Kangawa, K., Matsuo, H., Eto, T., Omae, T. Clinical studies on the sites of production and clearance of circulating adrenomedullin in human subjects. *Hypertension,* **1994**, *24*, 600-604.

[50] Nakayama, M., Takahashi, K., Murakami, O., Shirato, K., Shibahara, S. Induction of adrenomedullin by hypoxia and cobalt chloride in human colorectal carcinoma cells. *Biochem. Biophys. Res. Commun.*, **1998**, *243*, 514-517.

[51] Sugo, S., Minamino, N., Shoji, H., Kangawa, K., Kitamura, K., Eto, T., Matsuo, H. Interleukin-1, tumor necrosis factor and lipopolysaccharide additively stimulate production of adrenomedullin in vascular smooth muscle cells. *Biochem. Biophys. Res. Commun.*, **1995**, *207*, 25-32.

[52] Chun, T.H., Itoh, H., Ogawa, Y., Tamura, N., Takaya, K., Igaki, T., Yamashita, J., Doi, K., Inoue, M., Masatsugu, K., Korenaga, R., Ando, J., Nakao, K. Shear stress augments expression of C-type natriuretic peptide and adrenomedullin. *Hypert.*, **1997**, *29*, 1296-1302.

[53] Garayoa, M., Martinez, A., Lee, S., Pio, R., An, W.G., Neckers, L., Trepel, J., Montuenga, L.M., Ryan, H., Johnson, R., Gassmann, M., Cuttitta, F. Hypoxia-inducible factor-1 (HIF-1) up-regulates adrenomedullin expression in human tumor cell lines during oxygen deprivation: a possible promotion mechanism of carcinogenesis. *Mol. Endocrinol.*, **2000**, *14*, 848-862.

[54] Champion, H.C., Akers, D.L., Santiago, J.A., Lambert. D.G., McNamara, D.B., Kadowitz PJ. Analysis of responses to human synthetic adrenomedullin and calcitonin gene-related peptides in the hindlimb vascular bed of the cat. *Mol. Cell Biochem.*, **1997**, *176*, 5-11.

[55] Shirai, M., Shimouchi, A., Ikeda, S., Ninomiya, I., Sunagawa, K., Kangawa, K., Matsuo, H. Vasodilator effects of adrenomedullin on small pulmonary arteries and veins in anaesthetized cats. *Br. J. Pharmacol.*, **1997**, *121*, 679-686.

[56] Eguchi, S., Hirata, Y., Kano, H., Sato, K., Watanabe, Y., Watanabe, T.X., Nakajima, K., Sakakibara, S., Marumo, F. Specific receptors for adrenomedullin in cultured rat vascular smooth muscle cells. *FEBS Lett.*, **1994**, *340*, 226-230.

[57] Ishizaka, Y., Ishizaka, Y., Tanaka, M., Kitamura, K., Kangawa, K., Minamino, N., Matsuo, H., Eto, T. Adrenomedullin stimulates cyclic AMP formation in rat vascular smooth muscle cells. *Biochem. Biophys. Res. Commun.*, **1994**, *200*, 642-646.

[58] Feng, C.J., Kang, B., Kaye, A.D., Kadowitz, P.J, Nossaman, B.D. L-NAME modulates responses to adrenomedullin in the hindquarters vascular bed of the rat. *Life. Sci.*,**1994**, *55*, L433-L438.

[59] Venema, R.C., Sayegh, H.S., Kent, J.D., Harrison, D.G.. Identification, characterization, and comparison of the calmodulin-binding domains of the endothelial and inducible nitric oxide synthases. *J. Biol. Chem.*, **1996**, *271*, 6435-6440.

[60] Nishimatsu, H., Suzuki, E., Nagata, D., Moriyama, N., Satonaka, H., Walsh, K., Sata, M., Kangawa, K., Matsuo, H., Goto, A., Kitamura, T., Hirata, Y. Adrenomedullin induces endothelium-dependent vasorelaxation *via* the phosphatidylinositol 3-kinase/Akt-dependent pathway in rat aorta. *Circ. Res.*, **2001**, *89*, 63-70.

[61] Owji, A.A., Smith, D.M., Coppock, H.A., Morgan, D.G., Bhogal, R., Ghatei, M.A., Bloom, S.R. An abundant and specific binding site for the novel vasodilator adrenomedullin in the rat. *Endocrinology,* **1995**, *136*, 2127-2134.

[62] Lippton, H., Chang, J.K., Hao, Q., Summer, W., Hyman, A.L. Adrenomedullin dilates the pulmonary vascular bed *in vivo*. *J. Appl. Physiol.*, **1994**, *76*, 2154-2156.

[63] Christman, B.W., McPherson, C.D., Newman, J.H., King, G.A., Bernard, G.R., Groves, B.M., Loyd, J.E. An imbalance between the excretion of thromboxane and prostacyclin metabolites in pulmonary hypertension. *N. Engl. J. Med.*, **1992**, *327*, 70-75.

[64] Tuder, R.M., Cool, C.D., Geraci, M.W., Wang, J., Abman ,S.H., Wright, L., Badesch, D., Voelkel, N.F. Prostacyclin synthase expression is decreased in lungs from patients with severe pulmonary hypertension. *Am. J. Respir. Crit. Care. Med.*, **1999**, *159*, 1925-1932.

[65] Giaid, A., Saleh, D. Reduced expression of endothelial nitric oxide synthase in the lungs of patients with pulmonary hypertension. *N. Engl. J. Med.*, **1995**, *333*, 214-221.

[66] Sata, M., Kakoki, M., Nagata, D., Nishimatsu, H., Suzuki, E., Aoyagi, T., Sugiura, S., Kojima, H., Nagano, T., Kangawa, K., Matsuo, H., Omata, M., Nagai, R., Hirata, Y. Adrenomedullin and nitric oxide inhibit human endothelial cell apoptosis *via* a cyclic GMP-independent mechanism. *Hypertension,* **2000**, *36*, 83-88.

[67] Kim, W., Moon, S.O., Sung, M.J., Kim, S.H., Lee, S., So, J.N., Park, S.K. Angiogenic role of adrenomedullin through activation of Akt, mitogen-activated protein kinase, and focal adhesion kinase in endothelial cells. *FASEB J.*, **2003**, *17*, 1937-1939.

[68] Pietra, G.G., Edwards, W.D., Kay, J.M., Rich, S., Kernis, J., Schloo, B., Ayres, S.M., Bergofsky, E.H., Brundage, B.H., Detre, K.M. Histopathology of primary pulmonary hypertension. A